Catalysis Today 441 (2024) 114848

Contents lists available at ScienceDirect

Catalysis Today

journal homepage: www.elsevier.com/locate/cattod

Graphene-based materials for wastes, biomass and CO_2 valorization in catalysis: A technological perspective *via* molten salt synthesis

Sina E. Atakoohi [a], Elena Spennati [a,b], Paola Riani [b,c], Maria Paola Carpanese [a], Gabriella Garbarino [a,b,*]

[a] Università degli Studi di Genova, Dipartimento di Ingegneria Civile, Chimica e Ambientale (DICCA), Via Opera Pia 15, Genova 16145, Italy
[b] INSTM, UdR Genova, Via Dodecaneso 31, Genova 16146, Italy
[c] Università degli Studi di Genova, Dipartimento di Chimica e Chimica Industriale (DCCI), Via Dodecaneso 31, Genova 16146, Italy

ARTICLE INFO

Keywords:
Graphene
Molten salt
Graphite
Exfoliation
Top-down synthesis
Catalysis
CO_2 valorization

ABSTRACT

The exfoliation of graphite to graphene is one of the main methods of graphene production. In this paper, we provide an overview of the main molten salt methods for the exfoliation of graphite to graphene, including thermal and electrochemical exfoliation of graphite in molten salt. The fundamental mechanism of these methods is discussed in detail, along with the characterization techniques and instruments used to analyze the produced graphene. Additionally, the principles of eutectic salt mixtures, which play a crucial role in the exfoliation process, are discussed. The utilization of graphene-based materials in catalysis, particularly in the CO_2 and biomass valorization to produce sustainable fuels and chemicals, has been reviewed. The molten salt method is a simple and efficient way to produce graphene-based materials by using a molten salt medium to exfoliate the graphite. The purpose of this study is to provide a comprehensive overview of the current state of knowledge regarding the use of molten salt for the exfoliation of graphite to graphene, including their benefits and limitations.

1. Introduction

Graphene was discovered in 2004 by Andre Geim and Konstantin Novoselov, who received the 2010 Nobel Prize in Physics for their pioneering work based on micromechanical exfoliation. Since its discovery, graphene has become relevant in various scientific fields due to its unique properties [1–3]. Graphene is a one-atom-thick layer with sp^2 hybridized carbons in a hexagonal arrangement that has a large theoretical specific surface area of 2630 m^2g^{-1}, if fully exposed, which is about two orders of magnitude higher than graphite one (~10 $m^2\ g^{-1}$) [4,5]. Graphene is also known to have strong chemical resistance, excellent electrical and thermal conductivity, good dispersibility, self-lubricating properties, high thermal stability and mechanical strength while it is the thinnest and lightest compound ever discovered [5–7].

Given the mentioned properties of graphene, it stands as an interesting option for the field of catalysis. As environmental concerns grow due to the increasing concentration of CO_2 in the atmosphere, many researchers have focused on developing efficient, low-cost and green ways to produce sustainable fuels and chemicals [8–13]. With the idea of Power-to-Gas [14] and deep use of biomasses, these efforts are aimed at contributing to a net-zero energy cycle, wherein catalysis plays a crucial role. This would in principle allow to also upgrade biochar and carbon produced by rising technologies i.e., methane pyrolysis for turquoise H_2 production, dealing also with tunable synthesis for C-nanotube-based materials. In particular, in the frame of heterogeneous catalysis graphene-based materials have emerged as a promising class of catalysts due to their exceptional adsorption capability, large surface area, and tunable properties coupled with the ability to atomically distribute catalytically active species achieving single atom catalysts or hybrid materials where both a classical supported catalyst and a graphene-based phase are present [15–19], as indeed reported in recent literature review [20] for CO oxidation, CH_4 activation, 1,3 butadiene and acetylene hydrogenations and electrocatalytic reactions for oxygen reduction reaction and fuel cells applications [21].

The potential of graphene has resulted in various global research to

* Corresponding author at: Università degli Studi di Genova, Dipartimento di Ingegneria Civile, Chimica e Ambientale (DICCA), Laboratorio di chimica delle superfici e catalisi, Via Opera Pia 15, Genova 16145, Italy.
E-mail address: gabriella.garbarino@unige.it (G. Garbarino).

https://doi.org/10.1016/j.cattod.2024.114848
Received 31 January 2024; Received in revised form 23 April 2024; Accepted 27 May 2024
Available online 2 June 2024

promote, improve, and commercialize its production, and reports estimate that graphene demand will reach over 4100 tons/year by 2026 [22]. The available graphene synthesis processes can be grouped into two categories: top-down and bottom-up [23]. In terms of simplicity, efficiency, and influence on product qualities, each of the mentioned approaches offers its pros and cons. In bottom-up methods, carbon precursors, such as carbon-containing gases, biomass, and polymers, are converted to graphene using processes such as chemical vapor deposition (CVD), epitaxial growth, thermal pyrolysis, and direct organic synthesis. On the other side, in the top-down method, graphene could be simply produced by exfoliation of graphite mainly by mechanical, liquid-phase (LPE), electrochemical, and chemical (oxidation-reduction) exfoliation methods (Fig. 1)[21,24,25], as also extensively reported in the recent review by Yan et al.[26]. Because of requiring sophisticated infrastructure and operating conditions, bottom-up methods are usually more complicated and expensive compared to top-down methods; therefore, top-down approaches are classically considered more scalable [23,27], despite their low production yield and poor chemical conductivity materials. In general, to produce graphene from pristine graphite in top-down methods, it is necessary to overcome the sheet-to-sheet

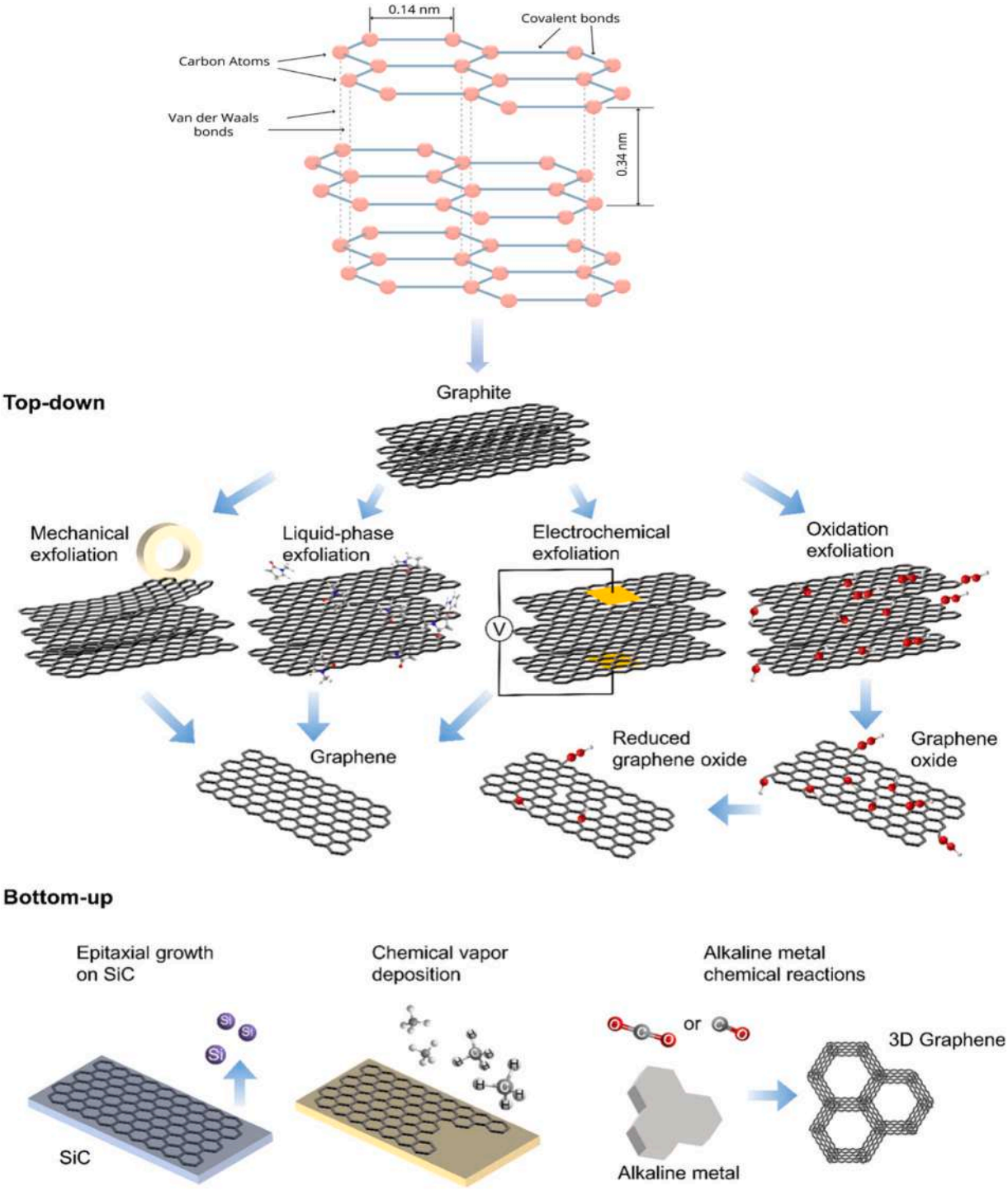

Fig. 1. Major synthesis methods of graphene.
Reprinted from ref [21] and slightly changed. Copyright: John Wiley and Sons, 2024.

interactions in graphite that are dominated by weak van der Waals forces (Fig. 1)[28].

However, also available top-down methods suffer from various disadvantages and challenges that limit full-scale graphene commercialization. The most commonly used top-down methods for producing graphene from graphite suffer from a longstanding quality vs. quantity tradeoff [29]. For instance, in the chemical exfoliation method, the Hummers technique is mostly used. It requires harsh and hazardous oxidizers such as H_2SO_4 and $KMnO_4$ and a complex synthetic route, with a final product that shows many damaged graphitic basal planes and formation of structural defects, being generally considered graphene oxide [30–32]. Among recent literature, a partial substitution of chemicals has been the object of investigation of different research groups dealing with $NaNO_3$-free Hummers method using K_2FeO_4, instead of by partly replacing $KMnO_4$, and controlling the amount of concentrated sulfuric acid [33] or recipe proposed in [34] where Tour's method[35] and modified ones have been tested. According to Tour's method, a treatment with hydrazine can produce Chemically Converted Graphene (CCG).

In mechanical exfoliation methods (ball milling is mostly used), the need for high energy, expensive devices, low yield, poor dispersibility, and long process time are the main reported problems[30,36,37], coupled with an increased number of produced functionalized unzip edges where some reactions might occur[26]. Electrochemical exfoliation approaches have several drawbacks such as limited yield, deterioration in the resultant graphene sheets, and production of graphene with more than four layers [25,38]. Liquid Phase Exfoliation (LPE), which is usually referred to as sonication in a liquid medium[37], is the least expensive method and, although promising, it has also some disadvantages such as low and inhomogeneous product yield, the use of harmful solvents, difficulties in separation of solvent from the product, damaged layers due to sonication/shearing, and time-consumption [36,39–41].

The above-mentioned approaches are always carried out in a liquid medium because it facilitates exfoliation via a controllable and homogeneous energy transfer to the graphitic material and it stabilizes the graphene product [42]. However, due to the hydrophobic nature of graphene-based materials, the liquid medium should contain surfactants [43] or special organics [44] to possibly improve the dispersion and as well limiting nanosheet reaggregation. However, the use of organic liquids is problematic due to their toxicity and their high boiling points (e.g., N-methyl pyrrolidone), which makes it difficult to isolate the graphene product and to remove impurities (e.g., surfactant) from the matrix [37,42]. Some studies investigated the optimum surfactant concentration and choices [43]. Among emerging alternatives, molten salt strategy could be the accounted as best solution both to take advantage of a liquid medium for the exfoliation of graphite, and to solve the problems of using organics, surfactants, and harsh chemicals. In recent years, the use of molten salts as a potential green media to produce graphene-like materials (by bottom-top approaches using pristine biomass) and graphene (by top-down approaches using pristine graphite) has attracted much attention [31,42,45–47]. As phase change materials (PCMs), with relatively low cost and no flammability, molten salts constitute a useful synthesis medium in a wide range of reaction temperatures by enhancing mass transfer rates, reducing the reaction temperature, providing a homogeneous heating media with strong ionic conductivity, and superior reaction kinetics with the production of a reduced amount of volatile and toxic chemicals [48–51]. In fact, molten salts can provide an inert medium for the occurrence of reactions without becoming directly involved in it and providing a uniform ionically conductive heating media. Moreover, the immersion of graphite into molten salt medium improves the graphite stacking order by closing the microcracks (known as Mrozowski cracks) [52–54]. As a further point, the nonaqueous nature of the molten salt enhances the dispersion of hydrophobic graphitic materials. Importantly, due to the high solubility of salts in water, the salt mixture can be easily removed from the product and regenerated, allowing good cyclability and reuse [50].

It is worth mentioning that, despite the potential of molten salt techniques, there are only a few reviews discussing the different synthesis strategies in molten salt medium and meanwhile devoted to catalysis applications. Moreover, their emphasis has mainly centered on different 2D materials and porous carbon production, rather than exclusively focusing on graphene [49,55–57]. Therefore, a comprehensive summary of the molten salt techniques to synthesize graphene-based materials from graphite (as a top-down approach), also considering the characterization methods, is still lacking. Also, the possible application in catalysis for the valorization of biomass and wastes poses the interest to shed light on the present topic evaluating strategies for possible use and exploitation in the catalytic field.

2. Application of molten salts to C-based materials

Molten salts [58] are recognized as suitable candidates for multiple purposes: high-efficiency heat transfer media in high-temperature partial oxidations, nuclear reactors, and concentrated solar power [59] applications, pyrochemical reprocessing of spent nuclear fuels, production of electrolytic carbon nanomaterials, molten media for turquoise H_2 production [60] and with the development of bubble column reactors[61,62], where deactivation is reported to be reduced, thermal vector fluid and heat storage system due to the high stability and low toxicity, and electrolyte for molten carbonate fuel cells [63]. As well, molten salts have been reported as a promising option in the activation of biomass to produce functionalized bio-carbons in single step thermal processes by mixing or immersion routes [64], or for the upgrading of wastes to produce fuels and chemicals[65].

In molten salt approaches to produce graphene and C-based materials, the eutectic system plays a crucial role. Eutectics have some characteristics of each pure phase but behave differently in terms of melting point, solubility, chemical stability, and salt purities [66–69]. Considering the mentioned advantages compared to a single salt, eutectic salt mixture has been used in most of the research related to preparation approaches to produce porous carbon and graphene-based materials. Table 1 lists the melting points of several salts and salt mixtures (eutectics) of practical interest to produce porous carbon and graphene-based materials.

2.1. Exploring Graphene-Based Materials and main characterization techniques

Theoretically, graphene is a monolayer of carbon atoms arranged in a honeycomb lattice which is also called single-layer graphene (SLG). Literature reports that the boundary between graphene and graphite properties is a layer number of 10; therefore, for graphite that has a layer number lower than 10, the term few-layer graphene (FLG) is generally used [74,75]. This is because the electronic structure changes with the

Table 1
Melting (T_m) and boiling (T_b) points of some metal chlorides and alkali hydroxides and their binary salt eutectic mixtures at atmospheric pressure [55, 70–73].

Salts	T_m (°C)	T_b (°C)	salt mixtures[(1)]	Molar ratio	T_m (°C)
$ZnCl_2$	290	732	$ZnCl_2$/KCl e	0.54 / 0.46	230
LiCl	605	1382	$ZnCl_2$/NaCl e	0.68 / 0.32	250
$MgCl_2$	714	1412	$ZnCl_2$/LiCl e	0.73 / 0.27	274
KCl	770	1420	KCl/LiCl e	0.41 / 0.59	353
$CaCl_2$	772	1935	$MgCl_2$/KCl e	0.30 / 0.70	423
NaCl	801	1413	$MgCl_2$/NaCl e	0.43 / 0.57	459
LiOH	471	924	$CaCl_2$/NaCl e	0.52 / 0.48	504
NaOH	318	1388	$CaCl_2$/KCl e	0.25 / 0.75	600
KOH	360	1327	KCl/NaCl az	0.49 / 0.51	657
KNO_3	334	400	LiOH/NaOH e	0.30 / 0.70	215
CsCl	646	1297	LiOH/KOH e	0.31 / 0.69	225
			NaOH/KOH e	0.51 / 0.49	170

(1) e stands for eutectic, az stands for azeotrope.

number of layers and, above 10 layers, approaches the one of graphite [2,76,77]. A comprehensive definition of various graphene-based derivatives has already been provided by Bianco et.al [74]. Furthermore, with graphene flakes which are produced by exfoliation of graphite, there will always be a distribution in thickness and in other general properties of graphene[78]. Therefore, quality determination and characterization are needed to control the exfoliation degree and efficiency of employed methods. Given the significance of determining the quality and characterizing graphene-based materials, it is essential to introduce various characterization techniques frequently applied in this field.

The most important technique for C-based material characterization is Raman spectroscopy, which is a powerful, fast, and generally non-destructive method. This technique provides information on the number and orientation of layers, the quality and types of edges, and the effects of perturbations, such as electric and magnetic fields, strain, doping, disorder, and eventual presence of functional groups [79,80]. The main features of graphene-based material obtained with Raman spectroscopy were already well studied and also discussed in many review papers [75,79–85].

As a key-point from cited works, the main features in Raman spectra of graphene-based materials are the G, D, and 2D (second order of the D) bands that upon a change in shape, position, and relative intensity, can reflect the evolution of the structural and electronic properties [84]. G band is due to the in-plane vibrational mode involving the sp^2 hybridized carbon atoms that comprise the graphene sheet. The position of the G band is highly sensitive to the number of layers[81]. The 2D band, which is always strong in graphene, is the result of a two-phonon lattice vibrational process. In addition to the G band, the 2D band provides information thanks to both the position also band shape, being related to the thickness of the graphene layer [79,81,84]. Furthermore, an indication on the number of layers can be determined by the intensity ratio of the G and 2D band or its full width at half maximum (FWHM) [83,86]. For instance, the ratio of I_{2D}/I_G bands for high-quality (defect-free) single-layer graphene is equal to 2 (Fig. 2.b)[81]. The difference between Raman spectra of graphite, and graphene, and the relation of bands with the number of layers is shown in Fig. 2.

The D band (known as disorder band) is due to the breathing modes of six-atom rings (Fig. 3.e) and appears when there are defects within the carbon lattice or due to the presence of amorphous carbonaceous phases in the structure of graphene [79]. Also, the edges can be always seen as defects when the laser spot includes them, even if the bulk sample is perfect, a D peak will appear (on edges, the D peak appears as two bands D_1 and D_2) [84,87]. The intensity of the D band is directly proportional to the level of defects [79,88,89]. Also, the ratio of I_D/I_G usually is used as an indirect estimation of the disorder in the graphene structure (Fig. 3.d)[90,91]. With these key principles in mind, Raman spectroscopy can be considered an essential tool for the characterization of graphene-based materials and, in the frame of heterogeneous catalysis, even though no examples are viable, the use of operando in the reaction conditions could allow following dynamic changes occurring at the catalyst upon reaction. Further comprehensive information regarding the fundamental principles of Raman spectroscopy in the characterization of graphene-based materials can be located within the references mentioned in this section.

As indeed obvious, several other techniques are used as a complement to Raman spectroscopy, and in particular various methods, including AFM, SEM, TEM, XRD, and XPS, play a significant role in the characterization of graphene-based materials, providing information on morphology, size, thickness, crystal structure, surface chemistry, and electronic properties, for the resonant Raman effect of π electrons in graphene [75]. Understanding the performance and limitations of each technique is crucial for accurate and thorough characterization of graphene-based materials. Techniques, such as atomic force (AFM),

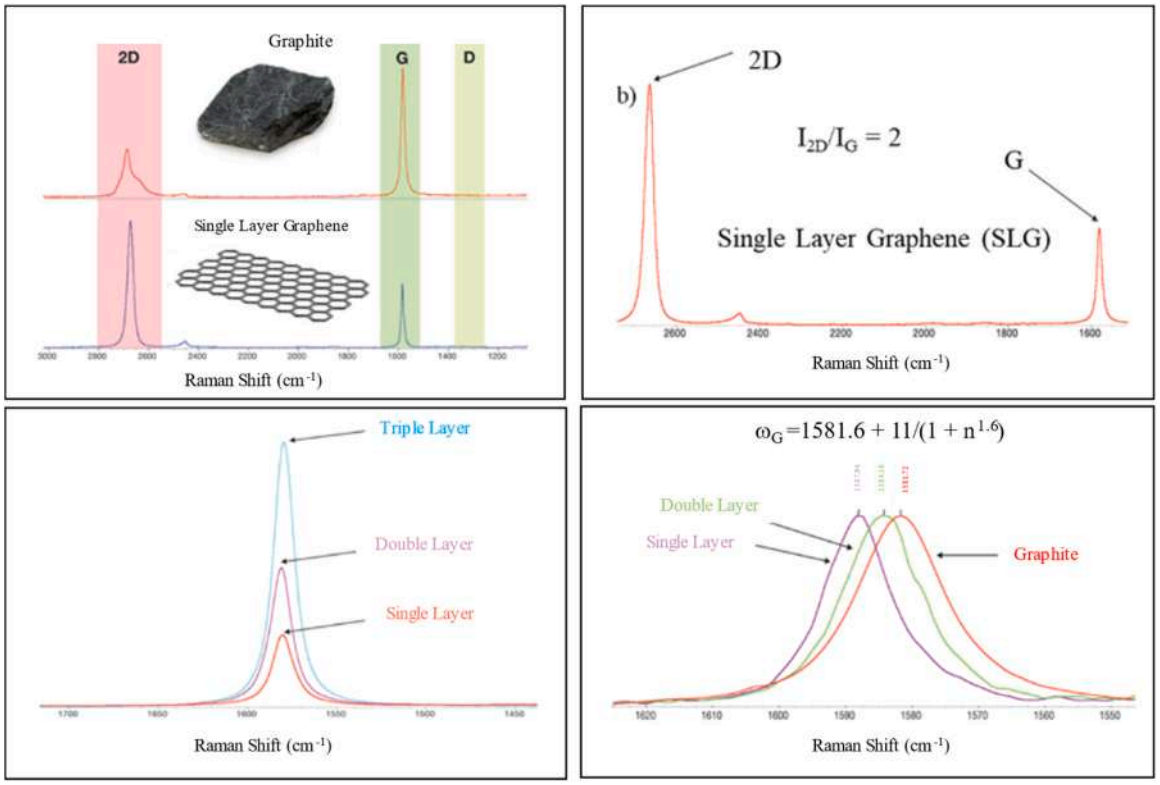

Fig. 2. (a) The Raman spectra of graphite and single layer graphene, collected with 532 nm laser wavelenght. (b) Single layer graphene can be identified by the intensity ratio of the 2D to G band. (c) There is a linear increase in G band intensity as the number of graphene layers increases, collected with 532 nm excitation. (d) The G band position as a function of layer thickness. As the number of layers increase the band shifts to lower wavenumber, collected with 532 nm excitation. Figures modified from ref [81].

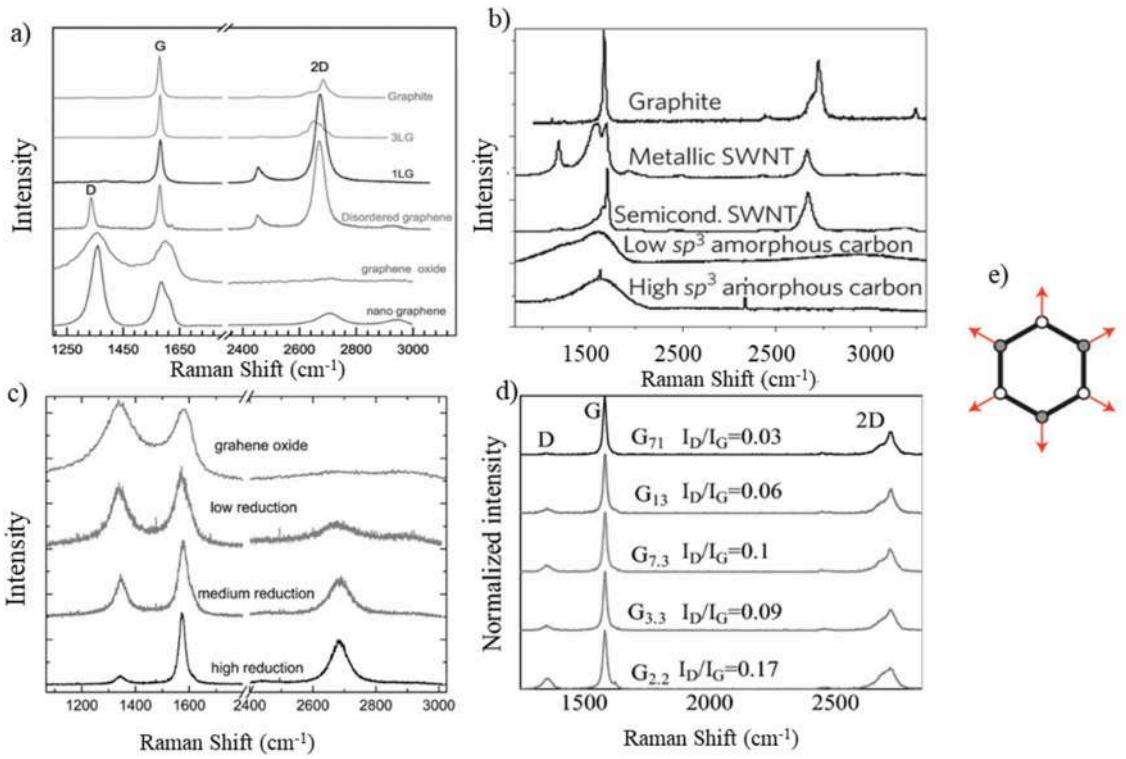

Fig. 3. (a) Raman spectra of graphene-based materials, including graphite, 1LG, 3LG, dis- ordered graphene, graphene oxide and nanographene[85].(b) Raman spectra of graphite, metallic and semiconducting carbon nanotubes, low and high sp3 amorphous carbons[84]. (c) Raman spectra from RGO at high, medium and low reduction, and GO[90] (d) Typical Raman spectra of different graphite samples [293]. I_D/I_G ratio is an average value for more than five data. (e) Atom displacements (red arrows) for the $A_{1\ g}$ mode at K[74].

scanning electron (SEM), and transmission electron (TEM) microscopies are the most used methods for the morphology, size, and thickness analysis of formed graphene layers. In particular, AFM can be used to produce 3D images of specimens, as well as physical characteristics such as surface morphology, roughness, and texture. However, with AFM it is difficult to accurately determine graphene thicknesses and layer number. TEM and SEM are frequently used to determine the number of layers in graphene flakes and the size of the formed graphene sheets [25,92, 93].

X-ray diffraction (XRD) can provide information on crystalline structures, micro-strain, crystallite size, and dislocation density [94,95]. Recently, it was used to determine layer numbers in graphene flakes [96]; obviously, it can also provide information on the reduction of GO to graphene (Fig. 4.a) [97]. Graphene surface chemistry characterization such as chemical states, elemental composition, empirical formula, and electronic state can be determined using X-ray Photoelectron Spectroscopy (XPS) [25,98,99]. XP spectra are obtained by irradiating a solid surface with a beam of X-rays and determining the kinetic energy of electrons that are emitted from the top surface of the material, allowing to quantify the density of defects via the O/C ratio, to assess various types of carbon functionalities, to identify the formation of chemical bonds, and to evaluate the physisorption of molecules [100, 101] (Fig. 4.b) [102,103]. In conclusion, a variety of microscopy techniques and X-ray-based methods exist for the characterization of graphene-based materials, each with its strengths and limitations.

In conclusion, a variety of microscopy techniques and X-ray-based

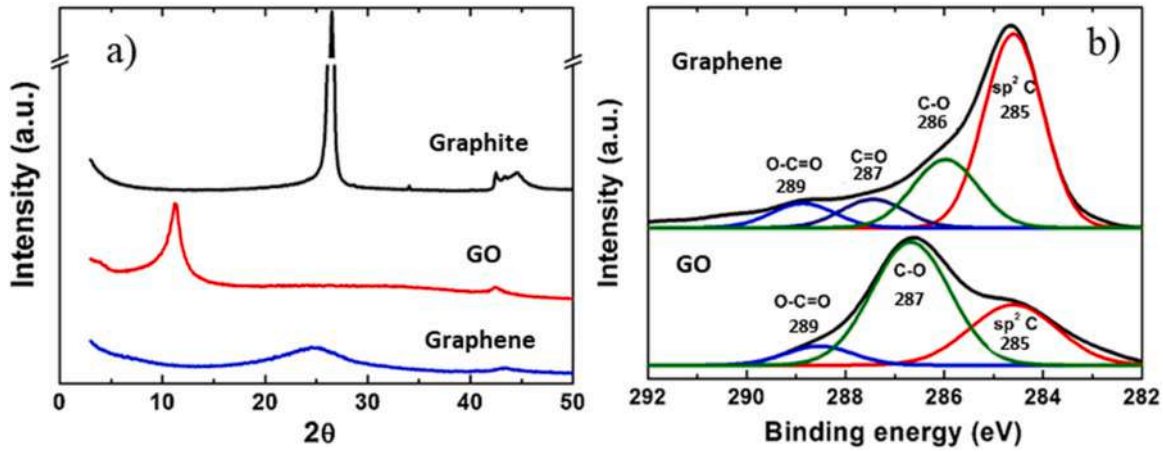

Fig. 4. XRD patterns of graphite, graphene oxide and graphene. XPS spectra of graphene oxide and graphene [98].

methods exist for the characterization of graphene-based materials, each with its strengths and limitations.

3. Thermal exfoliation of graphite in molten salt

As already introduced, molten salt provides a uniform inert reaction medium for the exfoliation process due to its excellent thermal storage and heat transfer ability. Since molten salt is a multipurpose reaction medium with a wide range of salt types and melting temperatures, it can be tailored to optimize the exfoliation of graphite into graphene with different properties based on the demanded applications [42,55], and produce graphene layers with a low number on defects through an economic and environmentally friendly process.

In 2013, Kamali and coworkers [104] were among the first ones who proposed a molten salt method for the corrosion of graphite as a possible way to produce carbon nanostructures. The experiment was simply done by heating a mixture of graphite powder and LiCl (46 wt%) to 1250 °C at different heating rates under a constant air flow rate of 100 mL min^{-1}. The result showed that high heating rates (80 °C min^{-1}) and the presence of molten LiCl can prevent the oxidation of graphite and, moreover it has been observed a strong increase in the graphite crystallinity that was usually observed at a temperature higher than 2500 °C. Furthermore, during this heat treatment, the intercalation of LiCl vapor, into the graphite structure, accounting for its reaction with Li_2O formed during the heating ramp and the catalytic decomposition of CO, led to obtain three distinctly different carbon microstructures: carbon sheets and nanosheets, pitted particles, and carbon nanorods (Fig. 5).

Later in 2014, Liang et al. [105] used molten hydroxides to synthesize graphene nanosheets from Graphite Fluoride (GF) at low temperatures. For this purpose, a eutectic mixture of KOH/NaOH was mixed with GF and heated to 160 °C for 4 h. After cooling down, the mixture was washed and exfoliated by an ultrasonication step in ethanol solution. After the phase separation, exfoliated graphene nanosheets with small amounts of oxygen functional groups were obtained.

In 2016, Xin et al. [106] performed a thermal treatment of a Flexible Graphite Sheet (FGS) in molten KNO_3 salt to obtain tuned carbon materials, like porous graphene. The process was started by melting anhydrous KNO_3 (T_m=334 °C) with a heating rate of 8 °C min^{-1} in an air flow rate of 100 mL min^{-1}. When the temperature arrived at the target of 350, 500, or 600 °C (it should be noted that decomposition of KNO_3 starts to KNO_2 at 650 °C [107]), FGS was added to the molten KNO_3 and kept for 12 h. After naturally cooling down to room temperature, the mixture was repeatedly washed with deionized water. XRD results (Fig. 6.D) show that the intensity of diffraction peaks decreased with temperature increase, revealing a crystal-to-amorphous transition. Likewise, Raman spectra (Fig. 6.F) indicate an increase in defect with temperature considering I_D/I_G ratios. At 350 °C, FGS was fragmented into graphene due to the intercalation of potassium ions into graphene layers (Fig. 6.A). At 500 °C, the increment of thermal energy causes the degradation of graphene to new morphologies like hollow carbon nanocages (Fig. 6.B). At the highest tested temperature i.e., 600 °C, amorphous carbon nanospheres were observed, which indicates that the regular arrangement of graphene layers has been damaged (Fig. 6.C). This has been justified by accounting that the two-dimensional graphene becomes thermodynamically stable by deformation in the third dimension to reduce the surface free energy [2]. Therefore, at higher temperatures, the regular lattice arrangement of graphene layers is damaged and deforms to carbon nanocages and other amorphous structures to minimize the surface free energy [106].

In 2020, Gürünlü et al. [31] used a eutectic composition of molten LiCl/KCl salts (45/55 wt%) to synthesize graphene from graphite at a temperature range of 500–800 °C, a heating rate of 20 °C min^{-1}, treatment time of 5 h, and a graphite/salt ratio of 1:10 in an inert environment by comparing with classical Hummer's method reduced material. Results showed that, with an increase in the temperature, particle sizes increased while, at XPS, the carbon content decreased. The obtained number of layers, using various characterization methods slightly differ. In fact, XRD and Raman data analysis proved that most of the produced graphene is FLG while based on the AFM analysis, only graphene produced at 600 °C is SLG, despite the discussed limit of the technique [25,

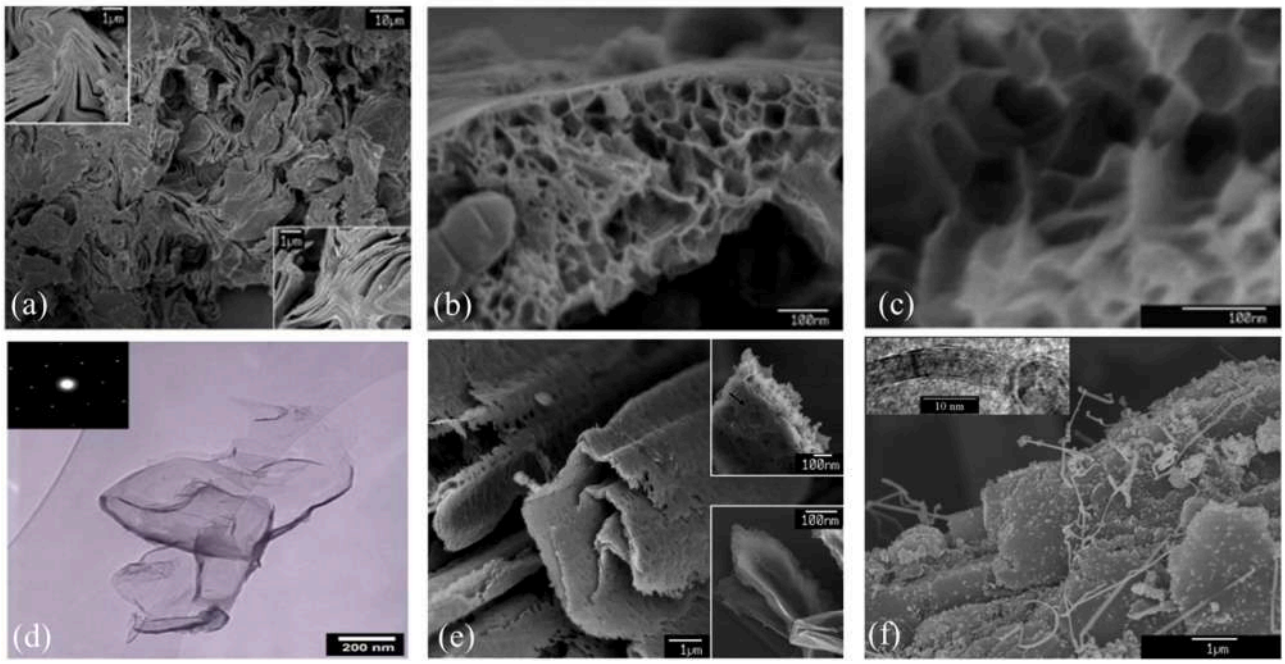

Fig. 5. Microstructure of the graphite–LiCl mixture heated at the rate of 80 °C min^{-1} to 1250 °C. (a) The dominant microstructure consisted of bent layered grains. (b) Exfoliated nanosheets which could be found in the microstructure. (c) TEM image of a graphene sheet. The inset is the selected area electron diffraction pattern taken from edge of the sheet showing the hexagonal structure of the (0001) basal plane. (d) The second microstructure comprises of corroded graphitic sheets. (e,f) The third microstructure comprising of carbon nanorods grown on the surface of graphite particles. [104].

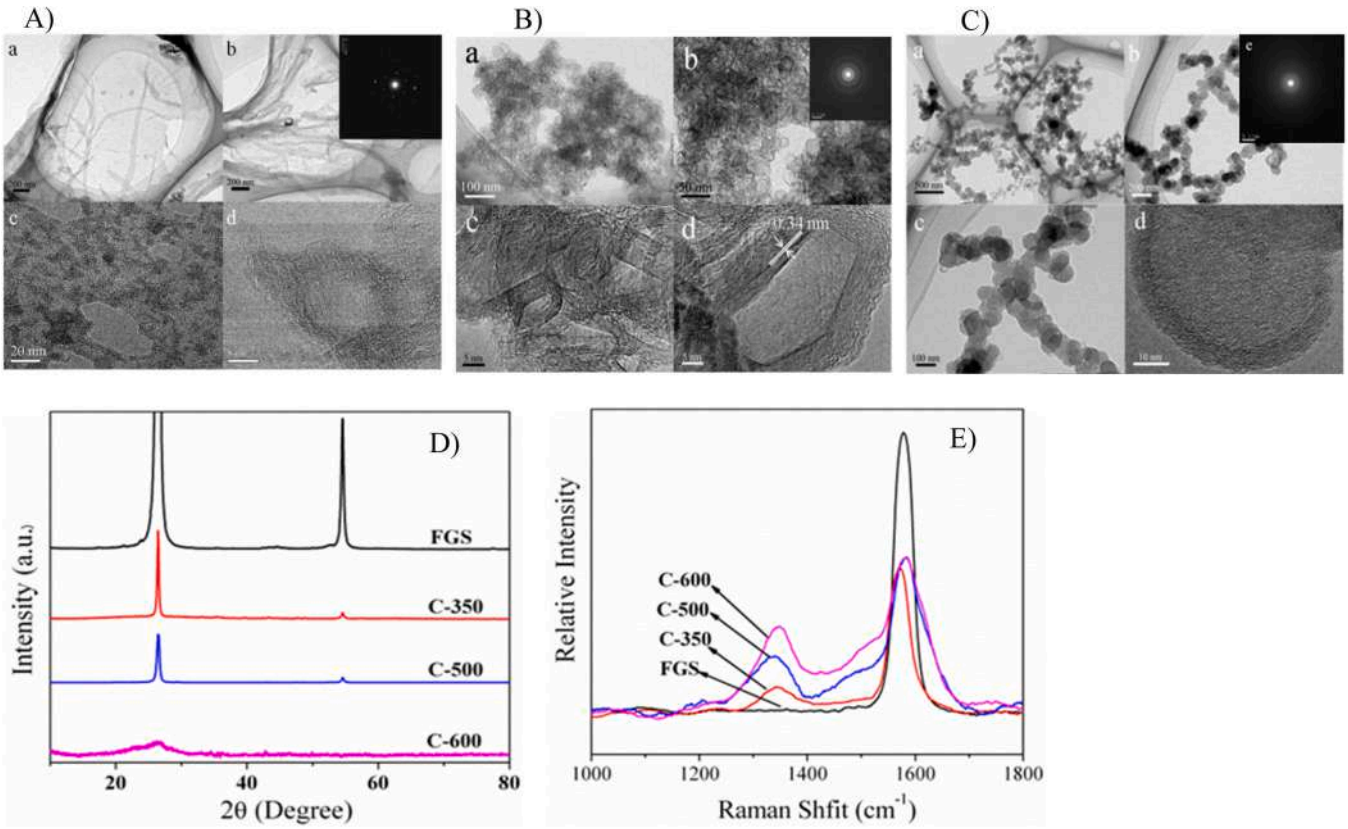

Fig. 6. TEM and SAED (Selected Area Electron Diffraction) pattern (in the inset) of C-350 (A), C-500 (B) and C-600 (C); XRD(D) and Raman spectra(E) of FGS, C-350, C-500, and C-600 figures (E) from ref [106].
Copyright: Elsevier, 2024.

92,93]. A summary of the results obtained by Gürünlü et.al [31] is reported in Table 2 with a maximum graphene conductivity at 600°C, in line with the detected number of layers.

Table 2
Summary of the results obtained by Gürünlü et al.[31].

Name	Particle size (nm)	Electrical conductivity (S/m)	I_D/I_G	Layer number from XRD results	Layer number from AFM results
Commercial graphene	2402	115	0.18	2	-
Commercial graphite	738	195	-	10	-
Reduced graphene oxide	4180	317	1.04	1	-
Graphene from graphite in molten salt media at 500°C	2660	1070	0.74	2	21
Graphene from graphite in molten salt media at 600°C	4205	1219	0.32	4	1–3
Graphene from graphite in molten salt media at 700°C	3017	803	0.11	2	21
Graphene from graphite in molten salt media at 800°C	3459	724	0.33	3	81

Despite the reported results [31], the use of LiCl might not be the best option due to the high demand and the scarce availability [108–110]. Recently, lithium has been set among raw critical materials in the frame of the energy transition scenario[111].

In 2021, Ruse et al. [42] performed molten salt in-situ exfoliation of graphite to graphene nanoplatelets (a few stacked layers of graphene form GnP [74,112]) in a NaCl/KCl azeotropic mixture in a 9:1 ratio with graphite and then heated with a rate of 10 °C min^{-1} in an argon flow of 50 mL min^{-1} up to 750 °C, and then treated with different residence time, in the range 30–360 min. After cooling down, the mixture was dispersed in ethanol and sonicated (at 0 °C) for 2 h, with a final phase separation and hot water washing. It has been evidenced that longer graphite treatment times in the molten salt increased GnP production due to an enhanced impregnation of salt into the graphite interlayers, achieving a yield of 30–40 %. Based on TEM and SEM, the GnP product displayed relatively large dimensions (12 μm), and low defect concentration based on Raman and XPS techniques.

In 2023, Lavi et al. [73] followed the same method proposed by Ruse et al. [42] but exploited the use of CsCl, NaCl, or KCl individually (or the NaCl/KCl azeotrope) as the molten salt media at a temperature of 850 °C. The authors investigated the effect of molten salt surface tension value on the result and reported that molten CsCl, which has the lowest value of surface tension among others, displayed the highest wettability of the graphitic layers, enhanced salt impregnation within the graphite layers, and hence facilitated total exfoliation of the graphite to GnP. Impregnation of salt within the graphite layers is shown SEM imaging in Fig. 7.

In the same year, Jalalabadi et al. [113] introduced an approach for exfoliating graphite into turbostratic carbon, a distinctive carbon class

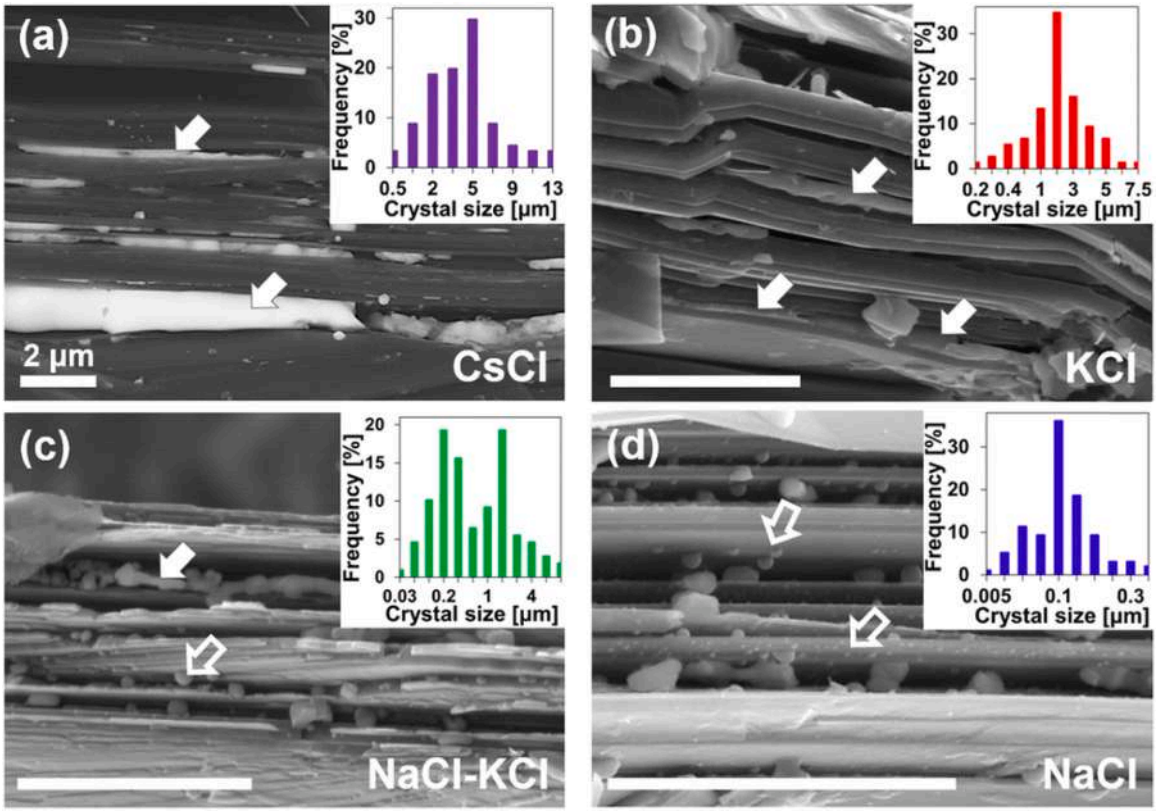

Fig. 7. SEM images, [73], of the GnP–salt composites obtained after treatment of graphite at 850 °C for 3 h in molten salts: (a) CsCl, (b) KCl, (c) NaCl–KCl, or (d) NaCl, showing nonwetting (small salt droplets, empty arrows) and wetting events in which the salt has impregnated within the graphitic layers (elongated salt crystals, full arrows). Scale bar = 2 μm. Upper right insets: size distribution (n = 100) histograms for impregnated salt crystals, as extracted from the SEM images. Copyright: Royal Society of Chemistry (RSC), 2024.

with structural ordering between amorphous carbon and crystalline graphite phases [114]. They used this eutectic mixture: Li_2CO_3 43.5 %, Na_2CO_3 31.5 %, and K_2CO_3 25 % (mole percentage), displaying a melting point of ~400 °C. In N_2 atmosphere, graphite to molten salt ratio, temperature (from 750 °C to 1000 °C), treatment time (from 1 h to 6 h), and pressure (5–10 bar) have been varied. By operating within a pressurized N_2 system, effective control over carbonate vaporization and decomposition has been achieved with an increase in exfoliation efficiency. Due to the intercalation of cations (Li^+, Na^+ and K^+) and possibly the anion (CO_3^{2-}) between graphitic layers, it was observed that the conventional d spacing of 0.34 nm (in graphite) is modified and expanded to a range of intervals between 0.41 nm and 1.22 nm. It is of interest to remark that the same authors also tested biochar producing a more amorphous carbon after the same treatment.

From the discussed works, it appears that the size of the cations and anions and molten salt wettability could play a crucial role in the exfoliation process, thus determining the efficiency of separation and the produced number of layers. In Table 3, a list of the most used salts and their relative ionic size can be observed.

According to the literature data, a preliminary summary of the reported mechanism can be briefly summarized for the sake of completeness. The energy of van der Waals forces between adjacent graphene layers in graphite structure is calculated as the sum of pair interaction potentials [118]. Generally, to separate graphene layers from bulk graphite, an applied external force must overcome the van der Waals attraction forces between adjacent graphene layers [37,119,120]. For this purpose, two methods can be considered: directly breaking the interlayer bonds or applying a shear force to slide away layer by layer.

Table 3
Ion size of the most used salts in the molten salt graphite exfoliation method.

Cation	Size(Å)Ref [115]	Anion	Size(Å)Ref [115–117]
Li^+	1.144	Cl^-	3.42
Na^+	1.886	NO_3^-	3.58
K^+	2.68	CO_3^{2-}	3.56
Cs^+	3.36	OH^-	2.66
Mg^{2+}	1.306	SO_4^{2-}	5.16
Ca^{2+}	1.942	Br^-	3.72

In a molten salt medium, ions may penetrate between the layers of bulk graphite material producing graphene layers. For instance, Xin et al. [106] reported that in molten KNO_3 media, potassium ions can penetrate graphite and exfoliate graphene sheets. By an increment of given energy, i.e. by molten salt media temperature increase, it can also be observed a degradation of graphene due to the occurrence of a redox reaction between carbon atoms and KNO_3 (Eq.1). This determines the careful need to choose the right molten salt for each of the wanted applications.

$$C+2KNO_3 \rightarrow KNO_2+CO_{2(g)} \quad (1)$$

The mechanism of exfoliation could change as a function of the chosen molten salt system. As an example, Ruse et al. [42] reported that no chemical reaction between the graphite and the NaCl/KCl azeotropic took place. The mechanism appears to be poorly investigated for molten salts, while it has been addressed in the case of water-salt solutions by identifying a central role for both the cation and the anion in facilitating the intercalation of more cation atoms in the inter-layer space by partially shielding the cation charge and even enhancing the intercalation in processes supported with ultrasonication [121–124].

According to the literature reports, simultaneously with the penetration of the ions, an exergy effect of cavities formed in molten salt helps to overcome the van der Waals forces and facilitates the exfoliation process. This mechanism lies on the variations of the salt crystalline

structure upon its melting and could justify the performance of molten salt media [42,125–129]. Upon the salt melting, each ion shows a short-range order with a number of first neighbor ions lower than the coordination number present in the solid state. According to [130–132], in the case of KCl/NaCl, the number of close neighbor cations (potassium or sodium) coordinating the chloride anions becomes 4, while the corresponding coordination number in the solid state was 6. The decrease of the number of first neighbor ions results in the formation of "cavities", whose diameter can be estimated at 0.6 nm [133], and that can occupy up to 20 % of the melt volume, thereby causing a reduction of the overall density [125–129]. Interestingly, with the dispersion in molten salt, the *d*-spacing of graphite increases (i.e. dispersing KCl up to ~0.6 nm, from 0.3 nm [134]). This expansion weakens van der Waals forces [118,135,136], therefore, cavities along with ions, penetrate and exfoliate graphene layers. The schematic of the mechanism is shown in Fig. 8.

Moreover, since molten salt creeps between graphite layers and remains there, after cooling, it aggregates in droplets within a process similar to Rayleigh instability[137] and crystallizes to salt particles. This process generates compressive stress on the graphitic layer which consequently improves the graphite stacking order by the closure of Mrozowski microcracks[52,53,138–140]. In this regard, Lavi et al. [73] recently proved that molten salts with a lower surface tension value could show better wettability of the salt towards graphite that ensure a high impregnation extent within the graphite layers (observable in Fig. 7) which leads to an increase of the graphitic stacking order.

As envisaged above, molten salt process generally applies gentle shear forces [42], while conventional Liquid Phase Exfoliation (LPE) of graphite provides extreme local conditions (effective temperature up to ~4727 °C, the local heating rates within a cavitating bubble ~10^{10}-10^{12} Ks^{-1}, local pressure ~20–30 MPa) by acoustic cavitation and implosive collapse of bubbles that apply both normal and shear forces (Fig. 9.a) [141–143]. Thus, the pressure required to separate two graphene sheets is estimated to be ~7.2 MPa [144]. Therefore, this severe condition due to local shock waves and microjets generated by collapsing cavitation bubbles (in the convectional LPE method) results not only in the exfoliation of the graphite but also in its significant fragmentation into small-sized graphene sheets and amorphous carbon[37,42,145](Fig. 9. *b*).

4. Electrochemical exfoliation in molten salt

Exfoliation of graphite may also be achieved by applying a potential to graphite (operated as an electrode) immersed in an electrolyte, which offers an alternative approach for the preparation of graphene-based materials, with the advantages of being more cost-effective, scalable, and environmentally friendly in comparison with other methods[146]. Graphite electrodes can be polarized either anodically (positive voltage) or cathodically (negative voltage). In anodic polarization, anions of the electrolyte intercalate into graphite anode and cause oxidation and possibly exfoliation. However, anodic polarization is usually kinetically slow and produces defective graphene due to over-oxidation of graphite [147]. In the cathodic process, where cations of the electrolyte are attracted to the graphite cathode, exfoliation can be conducted only by intercalation of cations into graphite without any oxidation; thereby, preventing of generation of defects in the product [148,149]. However, due less performant intercalation, the exfoliation efficiency of the cathodic process is lower than the anodic one [146].

The idea of electrochemical erosion of graphite in a molten salt electrolyte to produce nanocarbon materials started in 1995 [150–153], way before the pioneer work of Andre Geim and Konstantin Novoselov in 2004 [1] for the separation of single layer graphene sheets from graphite. Molten salts, as green exfoliation electrolytes, can provide a uniform heating media, high ionic conductivity, superior reaction kinetics, sufficient intercalated ions and, thereby, effective exfoliation that is competitive when compared with low-temperature electrolytes ones [46,48,49]. A schematic of electrochemical exfoliation of graphite in molten salt media and the difference between cathodic and anodic

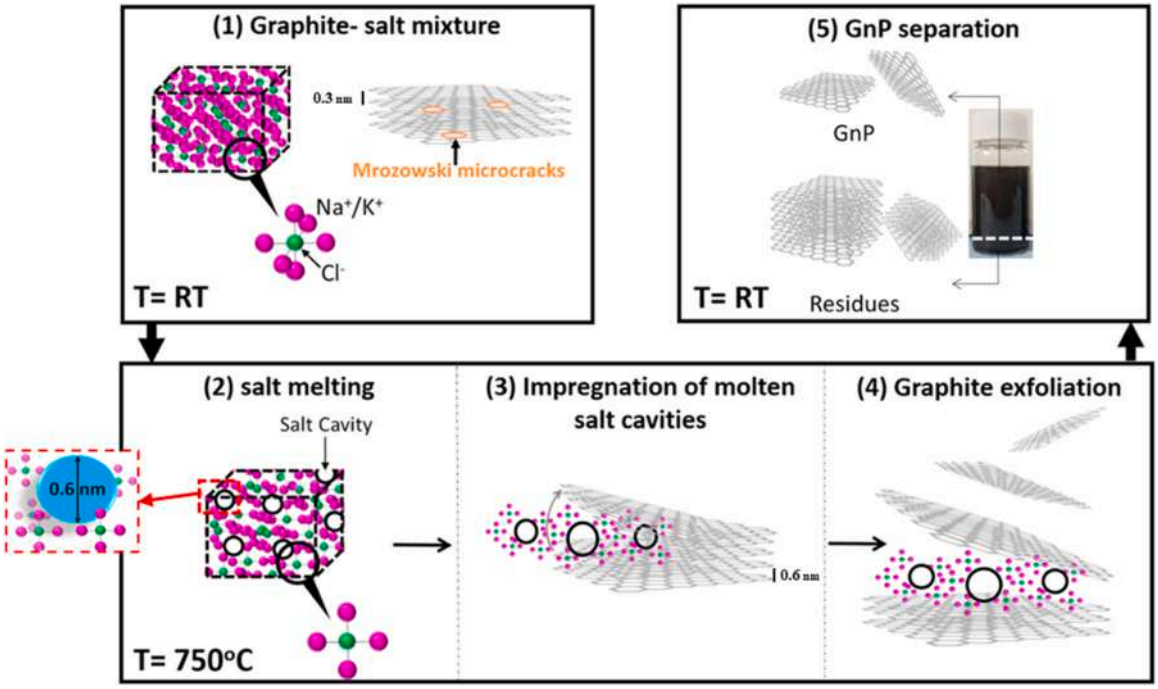

Fig. 8. Schematic illustration of GnP production in a molten azeotrope NaCl-KCl salt. Step (1) shows the starting mixture of graphite and solid salt. Step (2) heating the mixture to 750 °C and melting of the eutectic salt, leading to the formation of cavities in the salt (open black circles). Graphite exfoliation is initiated by graphite impregnation with the cavity-rich melt (step 3) and propagation of the cavities, which terminates in the formation of GnP (step 4). Step (5) separation of the GnP product at room temperature (RT) in ethanol. For simplicity, the ionic structure refers to both NaCl and KCl [42].

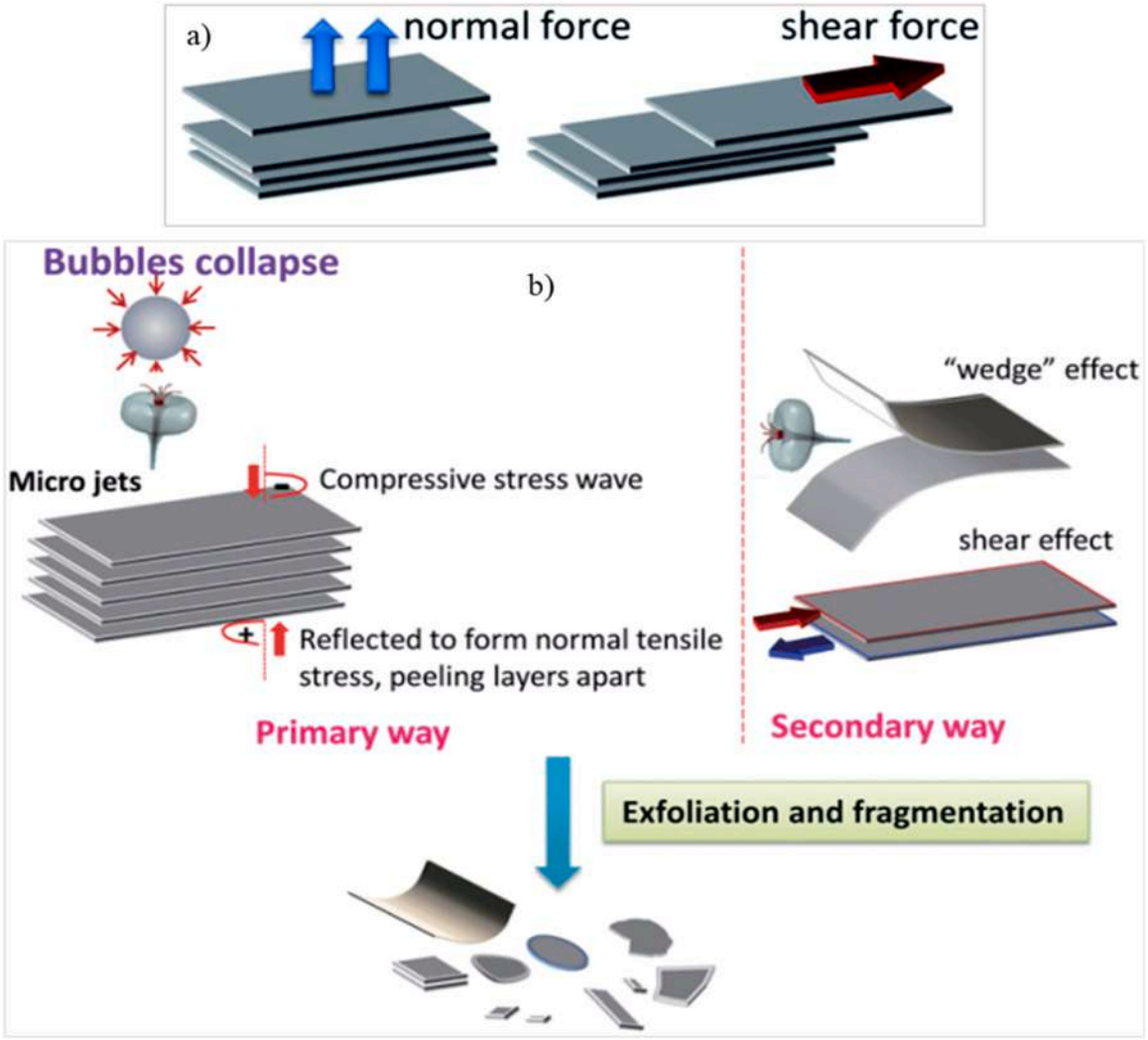

Fig. 9. a) Two kinds of mechanical routes for exfoliating graphite into graphene flake. b) The mechanical mechanism for exfoliation via sonication in convectional LPE methods [37].

methods is shown in Fig. 10.

Pure LiCl, LiOH, or a salt mixtures containing LiCl are mostly used to prepare molten salt electrolyte for electrochemical exfoliation of graphite [151–164], due to the relatively low melting temperature of LiCl (605 °C), or LiOH (471°C), and importantly, due to the small ionic radius of Li^+ (76 pm[165]) which facilitates the intercalation process.

In 2012, Huang et al. [160] were among pioneers in proposing a cathodic exfoliation of graphite to graphene in molten LiOH at 600 °C, by conducting a constant current of 15 A for 30 min, followed by a sonication process in water (Fig. 11). They reported a 80 % conversion of graphite cathode to few-layer graphene. However, it is worth to mention that cathodic exfoliation of graphite in LiCl medium generates a heterogeneous composition of various nanostructured constituents like particles, fibers, tubes, graphene species, and macroscopic graphite fragments that detached from the cathode without undergoing a reaction with the molten salt [150,152,156,157].

In 2015, Kamali et al. [158] reported that low-defect graphene nanosheets (I_D/I_G = 0.28) could be obtained in this way by adding humid Ar in a molten LiCl electrolyte. Thereafter, the same group in 2016 [163] investigated the cathodic exfoliation of graphite in molten LiCl by the novelty of introducing an Ar-H_2 atmosphere. The test has been performed in the following conditions: 800 °C with a heat ramp of 5 °C min^{-1}, under a flow of 200 cm^3 min^{-1} of a gas mixture Ar–4 %H_2 and applying a current of 40 A (corresponding to a cathode current density of 1 A cm^{-2}) and an average voltage of 5 V. The half-reactions occurring at the cathode (1) and the anode (2) accounting also for the consecutive anodic reaction in-between evolved Cl_2 and H_2, which is in the atmosphere above the molten salt, produces HCl (3).

The size of involved species allows them to intercalate into the van der Waals gaps between graphene layers.

Considering that HCl is highly soluble in LiCl-based molten salts, it dissolve and then ionize in the molten salt media, producing protons and chloride ions [166–168]. The formed H^+ are reduced on the graphite cathode and form hydrogen atoms which can intercalate into graphene layers of graphite electrode. Subsequently, the hydrogen atoms between the graphene layers form hydrogen molecules and further exfoliate graphite into high-quality graphene nanosheets (Fig. 12.).

Moreover, according to cited references, the process mainly proceeds by the cathodic discharge of H^+ and not Li^+. For comparison, they conducted the molten LiCl process under the same condition with the difference of using pure argon instead of Ar-4 %H_2 and concluded that the obtained products are mostly carbon nanotubes and nanoparticles and not graphene sheets.

Electrochemical exfoliation of graphite in molten LiCl showed promising results in the production of high-quality graphene; however, the above discussed limitations are actually considered as bottle-neck of

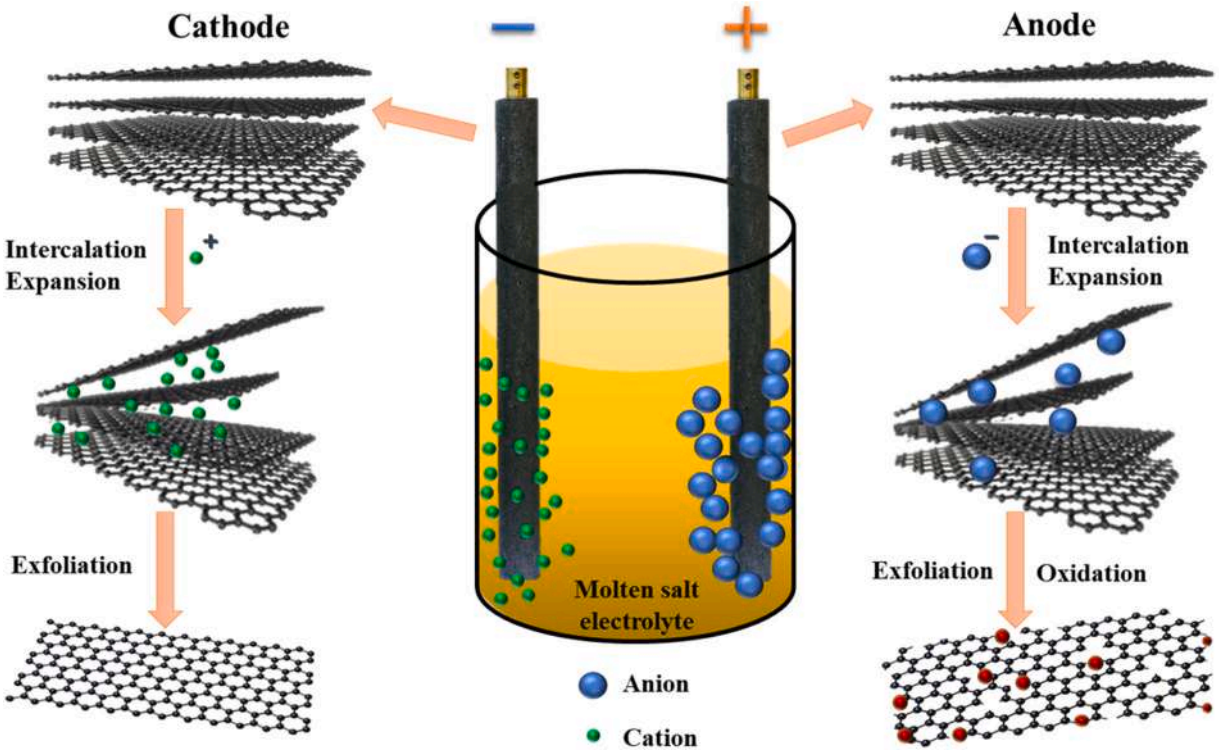

Fig. 10. Schematic illustration of mechanism of cathodic and anodic electrochemical exfoliation of graphite in molten salt electrolyte media.

the technology. In particular, the cost of lithium has risen from US$ 6000 per ton in 2020 to US$ 78,032 a ton in 2022, a 13-fold increase in less than two years[169]. Therefore, it was necessary to search for suitable replacements for LiCl.

In this regard, in 2017, Kamali et al. [170], proposed a modification of their original method [163] with the difference of using NaCl instead of LiCl as medium to produce highly conductive 3D graphene. The exfoliation was performed at 900 °C, above the melting point of NaCl (Table 1), with an Ar-4 %H_2 of 300 mL min^{-1} and using an electric current of 35 A for 120 min. Due to hydrogen intercalation into graphite and the effect of surface tension between graphene and molten NaCl, graphene nanosheets shaped into spherical configuration which then crumpled on each other to form balls (Fig. 13.a,b). The carbon balls were heated in a tube furnace under a flow of N_2-1 %H_2 to 1400 °C and held at this temperature for 3 h. Upon heating, and consequently, evaporation of NaCl the graphene balls tend to open up to form well-defined nanosheets (Fig. 13.c,d,e,f).

The production of graphene in molten NaCl is comparable with that in molten LiCl. Furthermore, sodium chloride is an economical and sustainable replacement with an average price of US$ 150 per ton[171] with almost an infinite amount (oceans with 36 thousand billion tons of dissolved NaCl), way greater than identified lithium resources (about 40 million tons)[172], even though high reaction temperature (above 1400°C) are required. Moreover, even though the boiling points of NaCl and LiCl are close, molten LiCl can be easily hydrolyzed in the present of moisture leading to faster evaporation of salt far below the nominal boiling point and thereby, increasing the corrosion rate [170,173].

Furthermore, various salts and eutectic mixtures were tested to produce graphene for distinctive applications [46,48,154,174]. In 2020, Yang et al. [46] proposed a simultaneous exfoliation of graphite on both cathode and anode in molten NaOH−KOH at relatively low temperature (300 °C). The advantages of this salt mixture lie not only on low melting point (eutectic point = 171 °C), but also in providing both alkali metal and hydrogen for anodic and oxygen for cathodic exfoliation, simplifying previous reported layouts. Furthermore, the operation at low temperatures could reduce the complexity and avoid product oxidation.

Although simultaneous cathodic and anodic exfoliation of graphite electrodes can significantly increase the graphene production rate, the quality, and properties of the generated graphene from cathode and anode could be different. Also, it has been reported that, by applying a constant voltage, cations and anions could accumulate between graphite layers suppressing the exfoliation process [38]. To solve these issues, Alshamkhani et al. [48] proposed a dual graphite electrode exfoliation in molten NaOH−KOH by using a switching voltage (12 V DC switching relay) technique. Results indicated that the switching voltage technique could positively affect the production of few-layer graphene with lower defects than that obtained upon constant voltage conditions.

Overall, electrochemical exfoliation of graphite in a molten salt electrolyte offers a cost-effective, scalable, and environmentally friendly alternative to other methods for the preparation of graphene-based materials. The use of suitable Li-free molten media or electrolytes and the application of switching voltages may achieve the production of high-quality graphene nanosheet, optimized for selected applications, but further research in this area is necessary.

To achieve a comprehensive overview, literature works that used molten salt method for the top-down production of graphene were summarized in Table 4.

5. Reduction of GO in molten salt

Graphene oxide (GO) is an oxidized graphene sheet randomly decorated with hydroxyl and epoxy groups. Therefore, GO can be considered a potential precursor to produce graphene. Due to the presence of oxygen, GO is not conductive even though, in principle, applying a reduction process, a conductive sheet of graphene can be obtained. In reality, reduced GO (rGO) typically has a lower electrical conductivity than its original material due to incomplete recovery of its π-π conjugated system [175–180].

Several reducing methods have been reported and briefly described in the following. Thermal reduction is a simple approach but the long time high-temperature treatment makes the process unaffordable and also causes damages to the structure of graphene [181,182]. On the

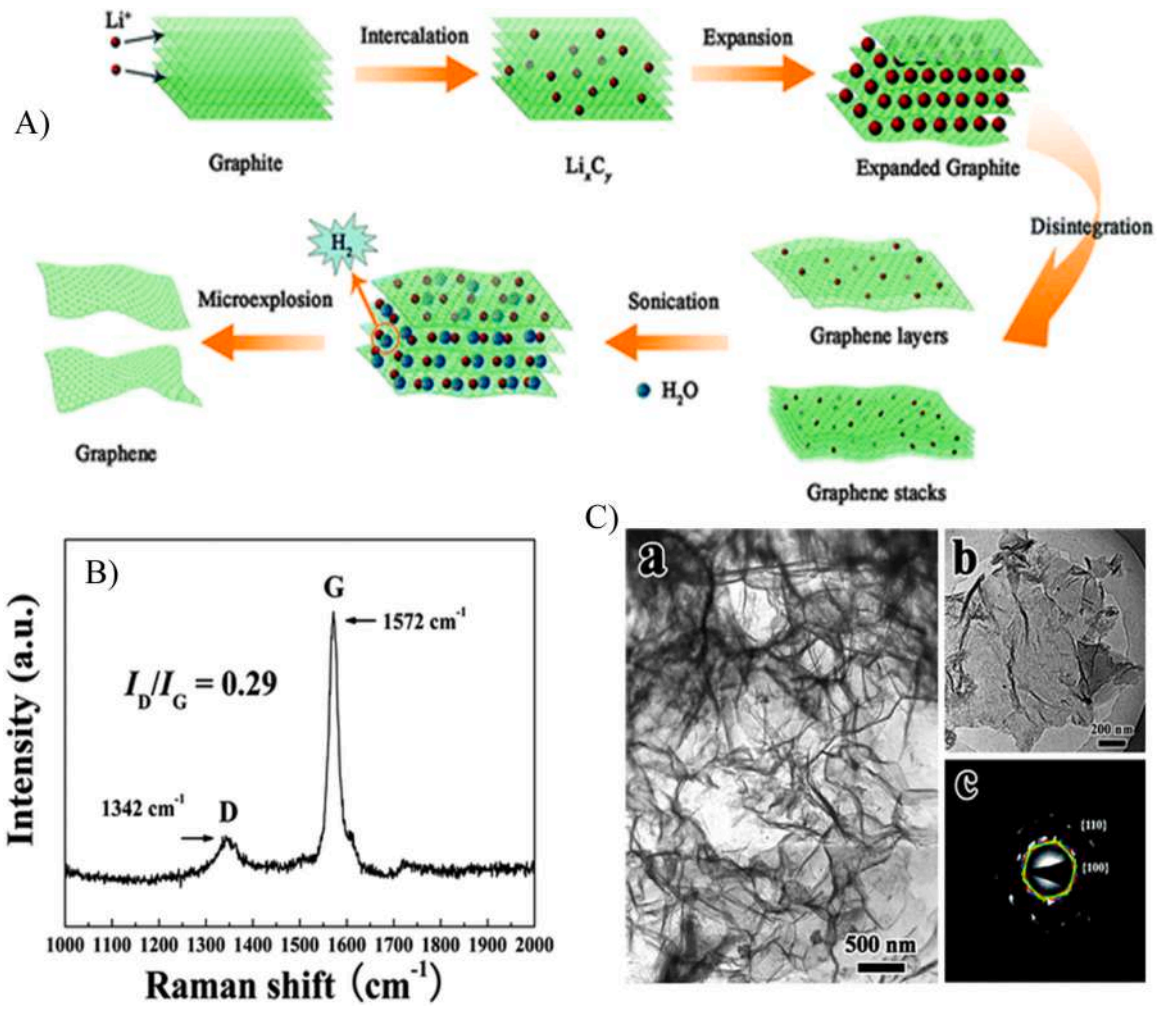

Fig. 11. A) formation steps of graphene sheets through Li intercalation–expansion–micro explosion process, B) Raman spectrum of the as-formed graphene nanosheet powders, C) (a) A low-magnification TEM image of many graphene sheets. (b) A high-magnification TEM image of the few-layer graphene sheets. (c) The corresponding SAED pattern in (b) [160].

other side, in wet chemical reduction, the involved reducing agents such as hydrazine [183], sodium borohydride [184], hydrogen sulfide [185], HI [186,187], hydroquinone [188], and dimethylhydrazine [189], are usually toxic and corrosive and may introduce additional functionalization during the reduction process itself [175,190]. Therefore, evaluating a replaceable green, and sustainable method to obtain rGO could be essential for many potential applications. Molten salt can offer an environmental-friendly route for the reduction of GO with the advantages of high yield, low cost, and short process time. Furthermore, it has been reported that the molten salt reduction method prevents restacking and restores the π-π conjugated network of graphene [176].

In this regard, Dilimon et al. [191], performed electrochemical reduction of exfoliated GO at room temperature, in a ternary eutectic melt of acetamide/urea/ammonium nitrate and found this method suitable for the reduction of GO. In 2014, Abdelkader et.al [175] produced GO by modifying Hummer's method and then successfully reduced it in a eutectic mixture of LiCl/KCl at 370 °C in an Ar flow for various process times of 1–8 h. Final rGO showed a good conductivity of 2400 S m^{-1} and a specific surface area of 320 m^2 g^{-1}. From Raman spectra, it is observable that an increase in the reaction time increases the reduction level of GO (considering that the signal of D band is shrinking while 2D band is getting more prominent).

Later, Abdelkader et al. [162] improved the reduction method [175] in the same condition but with the introduction of a constant cathodic voltage of 3.2 V. They obtained rGO with a specific surface area of 565 m^2 g^{-1} and the oxygen content was reduced from 30 % to less than 5 %. Wang et al. [176] reported a modified molten salt reduction method in which the oxygen functional group of GO can at once be replaced by nitrogenated groups to obtain nitrogen-doped graphene (NG). In this method, GO, KNO_3, and a eutectic mixture of LiCl/KCl were mixed with a weight ratio of 1:1:20 and heated to 600 °C in an N_2 atmosphere with a rate of 5 °C min^{-1} and held for 2 h. They successfully obtained a sp^2-hybridized NG with a deeply restored conjugated network with an I_D/I_G ratio of 0.81.

In 2018, Zhao et al. [190] recycled graphite from spent lithium-ion batteries to produce GO through a modified Hammer's method and then reduced it in a molten eutectic mixture of NaOH/KOH. The reduction was performed using a GO-salt ratio of 1:1 wt ratio in a Teflon test tube at 180, 220, and 300 °C for 10 h. Molten NaOH/KOH effectively eliminated the unsaturated oxygen-containing parts from GO sheets while creating more hydroxyl functional groups. Besides, an increase in temperature resulted in more disordered and more folded edges in the final rGO as observable in SEM analysis results and is in agreement with the work of Xin et.al [106]. The best results in terms of dispersion in water and ethanol were obtained at the process temperature of 220 °C.

In general, molten salt reduction of GO to rGO is a sustainable and green method and promising approach to produce graphene with

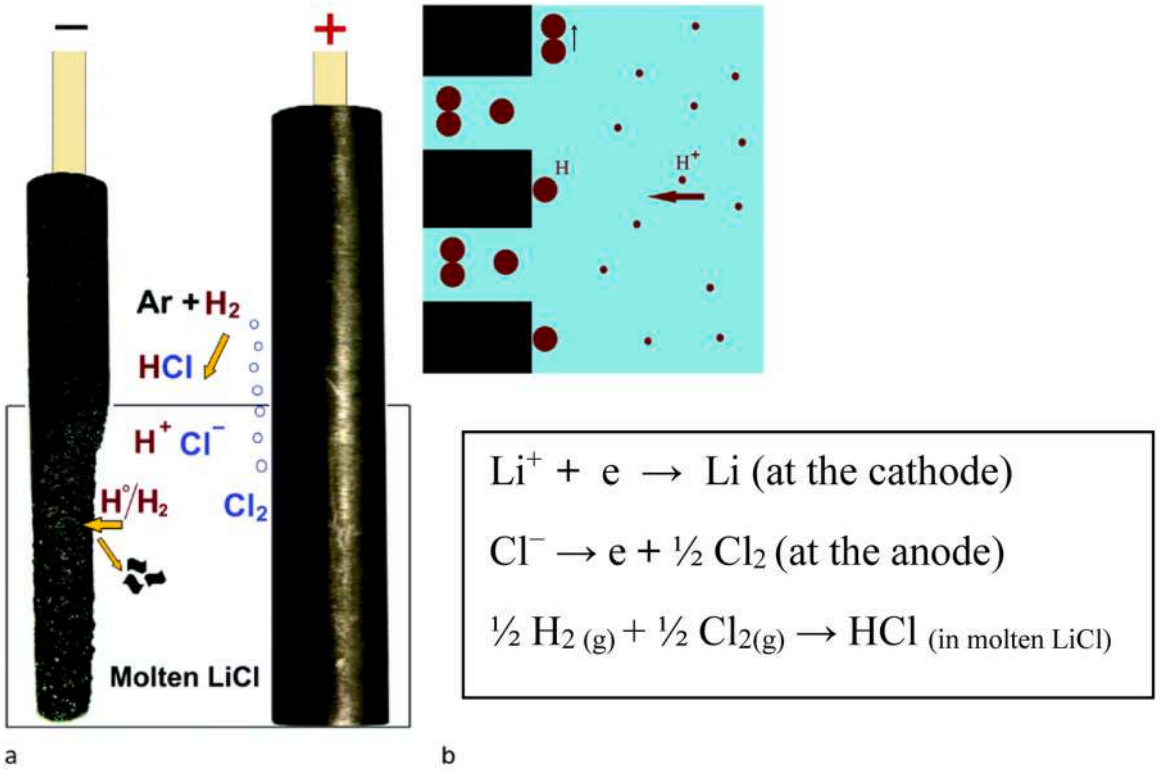

Fig. 12. Illustration of the mechanism involved in the preparation of graphene from graphite in molten LiCl in the Ar-H_2 atmosphere [163].
Copyright: Royal Society of Chemistry (RSC), 2024.

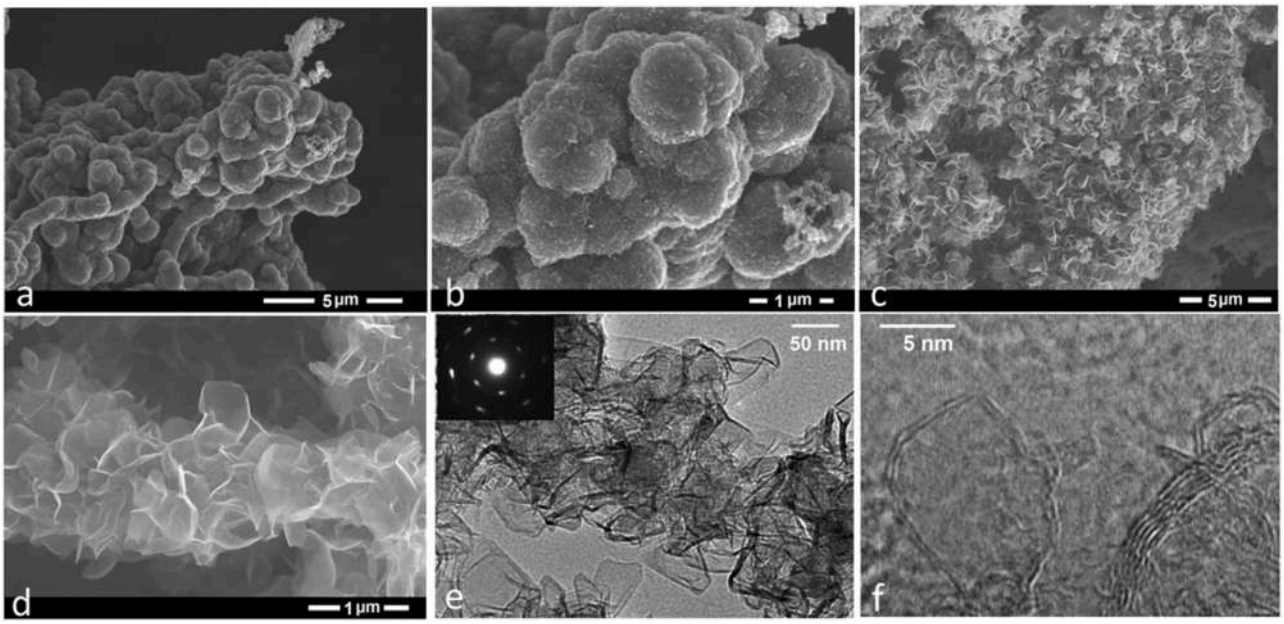

Fig. 13. Images of the carbon nanostructure produced by the exfoliation of graphite in molten NaCl (a,b SEM) followed by heating at high temperature (SEM c,d), TEM (e), and high magnification TEM micrographs showing that individual nanosheets are curved consisting of few atomic layers. The inset shows a typical selected area electron diffraction pattern recorded on the graphene material (f) [170].
Copyright: Elsevier, 2024.

improved electrical conductivity and specific surface area.

6. Pros and cons of molten salts method

In the following, the advantages and disadvantages of using Molten Salts (MS) methods in graphene-based material production are summarized.

Advantages:

- **Scalability** - it can be easily scaled up to produce large quantities of graphene.

Table 4
Molten salt methods in top-down production of graphene-based material.

Method	Carbon source	Molten salt	Atmosphere	T(°C)	Obtained product	I_D/I_G	Conductivity (S m^{-1})	No. of layers	P rate (g h^{-1})	Ref
ECE	Graphite rod	LiCl	Ar-Humidity flow	800	Graphene nanosheet	0.286	-	-	20	[158]
ECE	Graphite rod	LiCl	Ar	770	Carbon nanotubes	-	-	-	10	[161]
ECE	Graphite rod	LiCl	Ar–4 %H_2	800	Graphene nanosheet	0.400	-	1–10	19	[163]
ECE	Graphite rod	NaCl	Ar–4 %H_2	900	3D nanosheet	0.833	2.1 *10^5	-	8	[170]
DEE.cV.A	Graphite rod	Eu:KOH/NaOH	Air	300	Graphene nanosheet	0.216	-	1–10	26.9	[46]
DEE.cV.C						0.079	-	4–7	26.9	
DEE.cV	Graphite foils	Eu: acetamide, urea, NH_4NO_3	Air	ambient	Graphene	0.600	-	1–5	-	[174]
DEE. sV.A	Graphite pencil cores	Eu:KOH/NaOH	Air	300		0.650	75.28	10–11	30	[48]
DEE.sV.C					Graphene flakes	0.460	182.62	8	25.8	
DEE.cV.A						0.850	-	13–14	12	
DEE.cV.C						0.870	-	12–13	7.2	
ECE	Graphite rod	LiOH	Air	600	Graphene sheet	0.290	-	2–4	-	[160]
TE	Graphite powder	LiCl	Air flow	1250	Various carbon structures	0.060	-	-	-	[104]
TE	graphite fluoride	Eu:KOH/NaOH	Air	160	Oxygenated graphene nanosheet	~ 1–1.3	-	-	-	[105]
TE	flexible graphite sheets	KNO_3	Air	350	Graphene	~ 0.330	-	-	-	[106]
				500	Hollow carbon nanocages	~ 0.500		5–20		
				600	Carbon nanospheres	~ 0.660		-		
TE	natural flake graphite	Eu:LiCl/KCl	Ar or N_2	500	Graphene	0.740	1070	2	-	[31]
				600		0.320	1219	4		
				700		0.110	803	2		
				800		0.330	724	3		
TE	graphite	NaCl/KCl	Ar flow	750	Graphene nanoplatelet	~0.330	-	5–20	-	[42]
TE	graphite	CsCl/KCl/NaCl KCl/NaCl	Ar flow	850	Graphene nanoplatelet	0.100/ 0.100/ 0.040/ 0.040	-	5–20	-	[73]
TE	graphite	Mixture of: Li_2CO_3 Na_2CO_3 K_2CO_3	N_2, Atmospheric or under 5, and 10 bar pressure	750/800/ 900/1000	turbostratic carbon	-	-	-		[113]

Abbreviations: ECE, Electrochemical cathodic exfoliation; DEE, Dual-electrode exfoliation; cV, Constant voltage; A, Anode; C, Cathode; sV, switching voltage; TE, Thermal Exfoliation; Eu, Eutectic mixture

- **Reduced deterioration of final product** - MS methods can protect the quality and properties of the graphene by reducing the damaged graphene layers in the exfoliation process.
- **Low-cost** - MS could be an economical method for exfoliating graphite into graphene.
- **Salt recover and reuse** - in contrast to other methods, in MS technique the exfoliating medium (molten salt) can be recovered and reused within the production cycle. This can significantly reduce both the cost and environmental impact.
- **Environmental-friendly** - harmful chemicals are generally not involved in this method.

Disadvantages:

- Process parameters have a strong effect on the yield and quality of finally produced graphene.
- Equipment design could be delicate for possible corrosion processes occurring at high temperatures.
- The occurrence of side reactions and volatility of salts might hinder the industrial scale up.

7. Molten salt technique in biomass and plastic waste valorization

7.1. Biomass valorization

As previously noted, the bottom-up approach presents another possible method for producing graphene-based materials. However, in general, structuring graphene through bottom-up polymerization is more challenging and, consequently, has a restricted production rate [192]. Molten salt, apart from its application in the top-down approach for the synthesis of graphene-based materials from pristine graphite, can also be employed in a bottom-up concept, starting with a biomass precursor [57]. Biomass is commonly valorized into solid carbon (carbonization), liquid fuel, or gaseous syngas via thermochemical conversions (i.e., thermal hydrolysis, pyrolysis, and gasification) [193–196]. Carbonization typically induces polymerization by elimination of water, and frequently resulting in the formation of disordered carbonaceous matter [192]. On the other side, the carbonization of biomass in a molten salt medium has gained much attention in recent years as it opens new pathways for the conversion of biomass into high

added-value fuels and carbon materials [193,197]. The utilization of the molten salt method allows for the simplification of carbonization and activation into a single thermal step. Moreover, molten salts prove efficient in optimizing activation and regulating the pore structure of biochar. It can function both as a template and a catalyst for biochar activation. Additionally, it enables carbonization under an air atmosphere, facilitating the operational condition and promoting the O-doping onto biochar. Therefore, it not only acts as a protective medium to prevent carbon burning but also has the role of catalyst for carbonizing and activating biomass to generate porous carbons. Furthermore, the possibility of salt recycling, eases the scalability of this method [65,198–201].

In 2013, Liu et al. [192] were among the first reporting a controlled carbonization of glucose in a eutectic composition of molten LiCl/KCl for the synthesis of graphene. In the presence of ionic species, carbohydrates went through polymerization, producing nanoporous carbon with adjustable pore size. It has been observed that maintaining a low concentration of glucose, few-layer graphene is produced. Recently, Du et al. [202] reported the synthesis of porous few-layer graphene-like biochar by using kitchen waste as the biomass and molten K_2CO_3 as the carbonization medium. It has been concluded that the stacking of graphene layers and the development of a porous structure were affected by the volume of the reaction medium and the pre-carbonation of biomass. An increase in the dosage of molten K_2CO_3 favored the formation of a few-layered graphene structure, but an excessive quantity could present the adverse effect to disrupt the nanopore structure. A scheme of this process is shown in Fig. 14. Table 5 presents a list of recent studies exploring the utilization of molten salt for biomass valorization to graphene-based and carbon-based materials. The main method employed in these studies involves the pyrolysis of biomass in a molten salt medium, either in the presence of air or under an inert atmosphere depending on the specific application, but still poorly applied for catalytic ones. The resulting carbon-based materials in these investigations were predominantly utilized for applications such as supercapacitors, Li-ion battery anodes, adsorption, and oxygen reduction reactions (ORR).

Molten salt-assisted pyrolysis stands out as one of the promising methods for biomass conversion. This is attributed to its advantages such as faster mass and heat transfer, higher pyrolysis efficiency, superior product quality and scale-up potential, as well as simpler equipment and operation [55,56]. Nevertheless, a research gap exists in exploring the valorization of biomass into graphene-based materials using the molten salt method and its application in catalysis of CO_2 conversion to fuels.

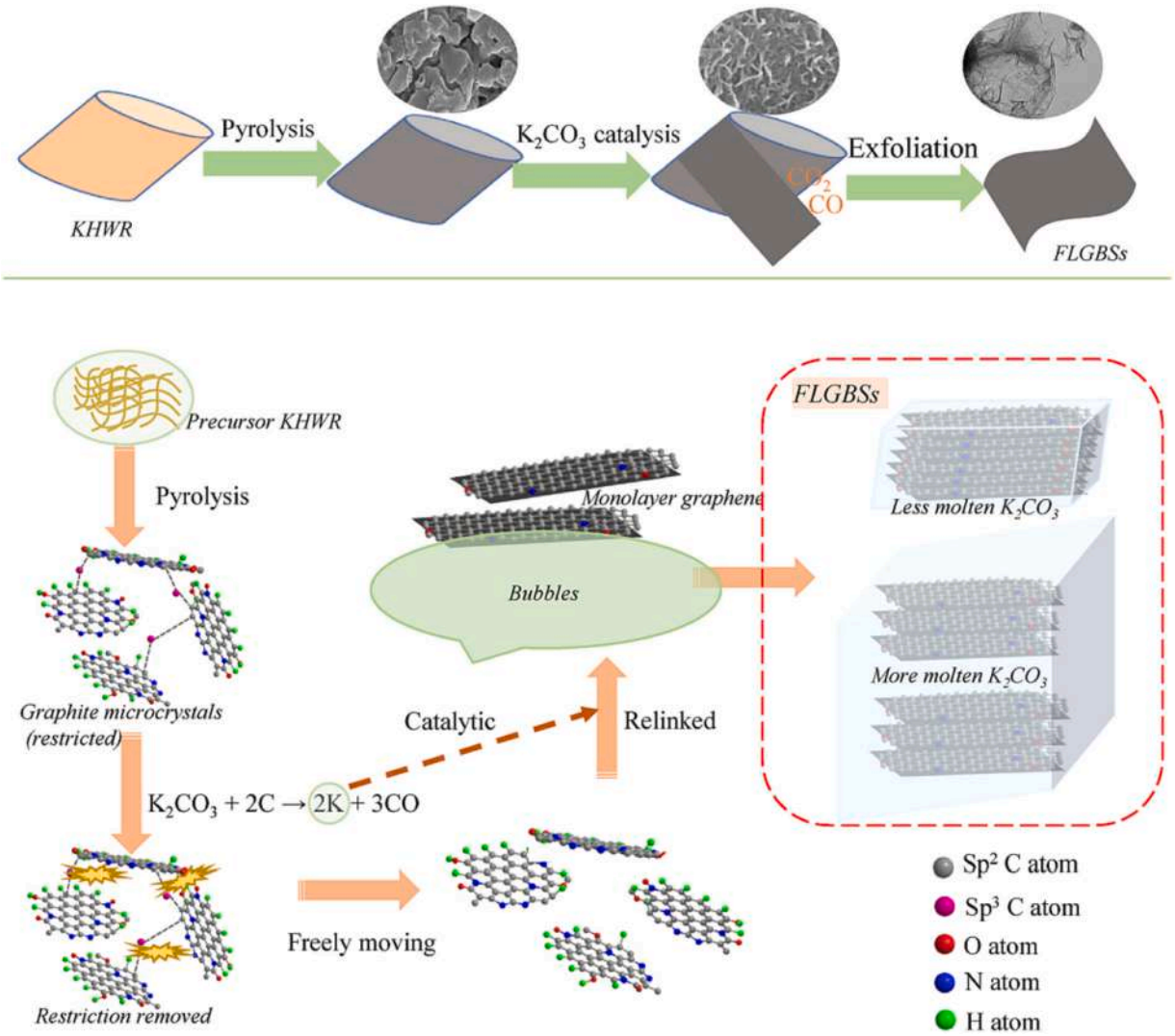

Fig. 14. Conversion of kitchen waste hydrolysis residue (KHWR) to graphene-like materials in molten K_2CO_3 medium [202].
Copyright: Elsevier, 2024.

Table 5
A list of recent research in the Molten salt-assisted valorization of biomass to added-value carbon-based materials.

Biomass	Molten Salt	Product	Ref.	Biomass	Molten Salt	Product	Ref.
Agaric	LiCl–KCl	Porous CNS	[203]	Wool fiber	LiCl–KCl–KNO_3	Hierarchical porous carbon	[204]
Bamboo leaves	$AlCl_3$	Hierarchical porous carbon	[205]	Milk powder	NaCl–Na_2CO_3	N-doped hierarchical porous carbon	[206]
Peach gum	NH_4Cl and $FeCl_2$	Heteroatom-doped porous carbon	[207]	Cornstalk	NaCl–KCl	Hierarchical porous carbon	[208]
Peanut shells	Na_2CO_3–K_2CO_3	Hierarchical porous carbon	[209]	Glucose	LiCl–KCl	CNT/ CNS	[210]
Kitchen waste	NaCl–KCl	N-doped porous carbon	[199]	Candida utilis	NaCl and KCl	N-doped BCNS	[211]
Rice husk	Na_2CO_3–K_2CO_3	Hierarchical porous carbon	[212]	Soybean meal	NaH_2PO_4 with NaCl–KCl	N, O, P co-doped hierarchical porous carbons	[213]
Lotus leaves	NaCl	N-doped layered graphitic biochar	[214]	Peanut shell	ZnCl2	Hierarchical porous carbon	[215]
Rice straw	K_2CO_3–Li_2CO_3	CuS-doped biochar	[216]	Wood sawdust	LiCl–KCl	Hierarchical porous carbon	[201]
Corncob	KCl/NaCl	S-modified porous biochar	[217]	Chlorella	NaCl/KCl	Carbon-supported single-atom catalysts	[218]
Chitosan	LiCl–$ZnCl_2$	N-doped hierarchical porous carbon	[219]	Coffee beans	Na_2CO_3–K_2CO_3 and $CaCl_2$	Porous carbon nanoflakes	[220]
Carrot	$ZnCl_2$	N and O enriched hierarchical porous carbons	[221]	Chitosan	$ZnCl_2$	Hierarchical porous carbon	[222]
Bamboo shell	Na_2CO_3–K_2CO_3	Hierarchical porous carbon	[223]	Clover stems	KCl	Hierarchical porous carbon	[224]
Chinese firewood	Na_2CO_3–K_2CO_3	Hierarchical porous carbon	[225]	Agaric	KNO_3/LiCl–KCl	N-doped CNT	[226]
Glucose	LiCl/KC	FLG	[223]	kitchen waste	K_2CO_3	FLGBS	[202]
Spirulina residues	NaCl/KCl/$ZnCl_2$	NBC	[227]	Rice husk	LiCl	Porous BC	[198]
PET waste	NaCl	Graphene nanostructures	[228]				

Abbreviations: FLG; few-layer graphene; NBC, nitrogen-doped biochar; PET, polyethylene terephthalate; CNT, carbon nanotube; CNS, carbon nanosheets; BCNS, biochar nanosheets; FLGBS, few-layer graphene-like biochar sheets

7.2. Plastic waste valorization

The growing pollution from plastic accumulation poses a significant threat to the environment and human health. In fact, the growing demand for bottled water has led to an annual consumption more than 500 billion plastic bottles. At this rate, the world will accumulate approximately 12,000 million tons of used plastic in the next 20 years [229–233]. Polyethylene terephthalate ($(C_{10}H_8O_4)_n$, PET, is commonly utilized in beverage and food packaging [234]; with a substantial carbon content of approximately 45 at% and the absence of inorganic, PET can be considered a viable source of high purity solid carbon materials [235]. The molten salt method can also be applied to upcycle plastic waste into valuable graphene-based materials [236].

In 1987, Bertolini et.al [237] conducted research on the use of molten NaOH-Na_2CO_3 to upcycle plastic waste, including polyethylene, polypropylene, polystyrene, and polyvinyl chloride. They found that pyrolysis in molten salts at low temperatures (420 °C – 480 °C) can reduce the gaseous fraction and produce valuable liquid and solid fractions, such as paraffin waxes and monomers. Pioneering the application of the molten salt for obtaining valuable carbon-based materials, Kamali et.al [238], were among the firsts to convert plastic waste, particularly PET from plastic bottles, into highly conductive nanostructured carbon. In the absence of salts, solid PET typically melts around 250 °C [146], decomposing in the presence of oxygen to produce gaseous species while leaving behind solid and dense carbon particles. On the contrary, when plastic material is heated with NaCl in air above the salt's melting point, the plastic undergoes melting and pyrolysis, resulting in the formation of amorphous carbon particles characterized by smooth surfaces and sharp edges. The molten NaCl then protects the carbon material from oxidation at higher temperatures and promotes its graphitization. This results in the formation of nanostructured carbon containing graphene-based nanosheets with high conductivity and surface area. The graphitization process begins around the edges of amorphous carbon particles at about 1100 °C and progresses as the temperature increases to 1300 °C. Finally, NaCl can be easily recycled and reused in the process.

Moreover, Kamali et al. [239] expanded their previous study by examining the impact of different molten salts, including KCl, $MgCl_2$, $ZnCl_2$, NaCl, KF, and NaF, on the structural and morphological changes of PET when heated in air to 1300 °C. They have reported that PET is transformed into carbon materials with different characteristics, including graphene-like nanosheets and porous nanostructures, with varying electrical conductivity values, depending on the type of salt employed. The melting and evaporation points, as well as the cation size of the salt, significantly influence the morphology and crystallization level of the carbon products, regulating the characteristics of PET-derived carbons. For instance, carbon materials generated in molten NaCl demonstrate high crystalline quality and electrical conductivity, boasting a S_{BET} of 702 m^2/g and electrical conductivity of 1354 S/m. In contrast, carbon material synthesized in $ZnCl_2$ exhibits the highest S_{BET} of 879 m^2/g but the lowest electrical conductivity at 9 S/m. Carbon materials derived from molten NaF and KF display reduced exfoliation, whereas those from molten $MgCl_2$ form highly porous carbon clusters and rolled graphene sheets. The possible mechanism involved in the conversion of PET into carbon nanostructures in molten salts is that when PET is heated with molten salt, the salt encapsulates the amorphous carbon particles left behind after the carbonization of PET. At high temperatures, the molten salt melts and covers the external surfaces and interval porosity of the carbon particles, leading to efficient graphitization and exfoliation of the material. The wettability of the carbon material with molten salts plays an important role in the penetration of the melt into the porosities, thus facilitating exfoliation and further graphitization of the carbon product. The crystallinity and graphitization degree of the carbon materials obtained in NaF, KF, and NaCl were considerably greater than those obtained in $ZnCl_2$, $MgCl_2$, and KCl.

The proposed molten salt process allows a significant positive environmental impact by converting plastic waste into high quality conductive carbon materials [146,236].

8. Application of graphene-based material in catalysis for CO_2 hydrogenation

Over recent years, to reduce the alarming net emissions of CO_2 in the atmosphere, attention has increasingly turned towards the hydrogenation of captured CO_2 by using green hydrogen. This method has gained

substantial interest as a possible way to enhance the value and recycle of carbon dioxide. These approaches show a great potential in reducing greenhouse gas emissions and promoting a sustainable energy cycle [8–13,240–243]. Available routes for the valorization of CO_2 involve its conversion into hydrogenated organic compounds, including methane, methanol, formic acid, synthetic fuels, etc.[244]. The respective reactions for these transformations are the following:

$$CO_2 + 4H_2 \rightleftharpoons CH_4 + 2\,H_2O \text{ Methanation} \quad (1)$$

$$CO_2 + H_2 \rightleftharpoons CO + H_2O \text{ reverse Water Gas-Shift (rWGS)} \quad (2)$$

$$CO_2 + 3H_2 \rightleftharpoons CH_3OH + H_2O \text{ Methanol synthesis} \quad (3)$$

$$(2\,n + 1)\,H_2 + n\,CO \rightleftharpoons C_nH_{2n+2} + n\,H_2O \text{ Fischer-Tropsch} \quad (4)$$

$$CO_2 + H_2 \rightleftharpoons HCOOH \text{ Formic Acid synthesis} \quad (5)$$

The existence of active and selective catalysts for CO_2 hydrogenation significantly contributes to enhancing process efficiency and industrial advances are reported in recent review work [245]. Conventional catalysts are primarily based on noble or non-noble transition metals, metal oxides, or hybrids that might face limitations due to high costs, toxicity, and environmental concerns [15,246]. Additionally, the tendency of metallic particles to aggregate due to their high surface energy often results in the loss of accessible active sites, leading to a reduction of catalytic activity and/or selectivity. Therefore, over recent years, several catalytic materials have been explored as potential alternatives to relieve the dependency on metallic resources to balance efficacy, efficiency, sustainability, and cost[15,17,19,246,247]. Recently, the promising properties of graphene have been applied to support the catalysis of different reactions [35] as well as for graphene-based materials. Its exceptional adsorption capability is particularly crucial in heterogeneous catalysis, serving as a fundamental requirement for reactant molecules to adsorb onto surface active sites and initiate then the formation of transition complex (reaction event). Furthermore, its simple structure promotes the simple diffusion of reactants to active sites, simplifying mass transfer without internal diffusion barriers [247,248]. Consequently, the interest in graphene-based materials for catalytic hydrogenation of CO_2 has significantly increased in recent years. Table 6 provides a list of the recent research in the available literature on the use of graphene-based catalysts for CO_2 reduction to methane, carbon monoxide, methanol, formic acid, and other useful hydrocarbons. It is interesting to notice that, in several cases, graphene-based materials are introduced in conventional metal-supported materials, giving rise to hybrid materials.

Some of the works listed in Table 5 have been discussed, and their key findings are outlined below. A recent study by Zhong et.al [249] investigated the suitability of Gnp as a support for cobalt-based catalysts (5 wt% Co/Gnp) in CO_2 methanation at low temperatures. Their findings revealed that cobalt supported on Gnp exhibited significantly enhanced performance in CO_2 methanation compared to cobalt supported on gamma-Al_2O_3. Gnp support facilitates the formation and sustenance of the active CoO phase on the catalyst surface, thereby boosting its reactivity for CO_2 methanation.

Méndez-Mateos et.al [264] investigated the influence of different supports, including GO, rGO, aminated GO, and alumina, on the performance of nickel-based catalysts in the methanation reaction. Graphene-based catalysts, especially rGO, showed enhanced activity in methane formation. Moreover, the ability of GO-derived material in heat conductivity, likely lead to a slight reduction in hot spot formation and improved temperature uniformity within the catalyst. However, they exhibited temperature sensitivity and tendency to deactivate at higher temperatures, limiting their possible application. In contrast, alumina supported catalysts presented superior thermal stability and resistance to deactivation. Comparisons showed that rGO-based catalysts yielded higher methane than alumina-supported catalysts indicating its potential to be used as a support for nickel catalysts in CO_2 methanation.

Table 6
A list of graphene-based catalysts for CO_2 hydrogenation to methane, methanol, formic acid, and other added-value hydrocarbons.

Catalyst	Application	Ref.	Catalyst	Application	Ref.
Co/GnP	Methanation	[249]	Pd_3Ni_5/CNT-rGO	Formic acid	[250]
Ni/rGONi/CeO_2-rGO	Methanation	[251,252]	$Pd_xAu_{(1-x)}$/PDA-rGO	Formic acid	[253]
			$Pd_{0.49}Au_{0.51}$/rGO	Formic acid	[254]
			SiG	Formic acid	[255]
Ni/GA	Methanation	[256]	Co/rGOLaCo/rGO	WGS	[257]
NGQDs/Al_2O_3	Methanation	[258]			
Ni/CNF-FLG	Methanation	[259]	Fe_x-Co_y/NG	rWGS	[260]
Ni@NGNi@G	Methanation	[261]	Fe3C/Fe@G	rWGS	[262]
			CuO-ZnO-ZrO_2-rGO	Methanol Synth.	[263]
Ni/rGO Ni/AGO Ni/BGO Ni-Ol/GO & Ni/Ol-GO	Methanation	[264]	CuO-ZnO-Al_2O_3-rGO	Methanol Synth.	[265]
			CuZnO/rGO	Methanol Synth.	[266]
			CuO-ZnO-rGO(3D)	Methanol Synth.	[267]
			CuO-ZnO-N-rGO(3D)	Methanol Synth.	[268]
Co/rGO(3D)	Fischer-Tropsch	[269]	Cu-ZnO-rGO	Methanol Synth.	[270]
FeK/G(3D) FeK/rGO	Fischer-Tropsch	[271]	CuO-ZnO-N-rGO	Methanol Synth.	[268,272]
			CuO-ZnO-ZrO_2-Al_2O_3-rGO	Methanol Synth.	[273]
FeK/G(3D)/HZSM-5	Fischer-Tropsch	[274]	CuO-ZnO-Al_2O_3-N-rGO	Methanol Synth.	[275]
Co/GnSCo−Ru/GnS	Fischer-Tropsch	[276]	Cu-Ni-rGOCu-Ni-N-rGO	Methanol Synth.	[277]
Co/G	Fischer-Tropsch	[278]			
Co/rGORh/rGO	Fischer-Tropsch	[279]			
Co-Ru/NGA	Fischer-Tropsch	[280]			
Co/GnSCo/N-GnS	Fischer-Tropsch	[281]			

Abbreviations: GnP, Graphene nanoplatelets; GA, graphene aerogel; NGQDs, Nitrogen-doped graphene quantum dots; AGO, Aminated graphene oxide; BGO, Boron doped graphene oxide; Ol-GO, Oleylamine aminated graphene oxide; NGA, Nitrogen-doped graphene aerogel; GnS, Graphene nanosheets; SG, Silicon doped graphene

Deerattrakul et.al[272] investigated the synthesis and evaluation of supported Cu-Zn/rGO catalysts for CO_2 hydrogenation to methanol. They found that the supported rGO nanosheets significantly improved catalytic performance by enhancing dispersion of Cu-Zn particles. They have also reported that graphene derivative's unique properties, including high theoretical surface area, tensile strength, thermal conductivity, and electron mobility, make it an excellent catalyst support material. The high surface area facilitates surface interactions and chemistry, while its mechanical properties and thermal conductivity contribute to catalyst stability and efficiency. The study concluded that supported rGO nanosheets enhance Cu-Zn catalyst performance, resulting in the highest space-time yield of methanol production.

Peng et al. [260] investigated the preparation of N-doped graphitic carbon supporting Co-Fe clusters using biomass waste for rWGS reaction. Their study revealed that sub-nanometric Co-Fe clusters supported on N-doped graphitic carbon exhibited high activity and selectivity toward CO. They also reported that N-doped graphitic carbon facilitated the preparation of clusters and small mono and bi-metallic nanoparticles, resulting in remarkable rWGS selectivity and higher activity compared to catalysts of larger particle size. On the contrary with SiO_2

support Co-Fe clusters showed significant differences in selectivity toward methane.

Alinia et.al [276] investigated the impact of different catalyst supports γ-Al_2O_3, CNT, and GNS on cobalt and cobalt-ruthenium catalyst performance in Fischer-Tropsch synthesis. They reported that those supported on GNS exhibited high surface area and improved reduction, leading to enhanced dispersion, smaller crystal sizes, and higher reduction rates of cobalt particles. Moreover, GNS-supported catalysts exhibited superior performance, with higher carbon monoxide conversion rates (64.5 % increase in CO conversion compared to γ-Al_2O_3 and a 25.9 % increase compared to CNT) and increased selectivity for C_{5+} hydrocarbons compared to γ-Al_2O_3 and CNT.

Vallejo Narváez et al. [255] carried out a molecular simulation study to examine the catalytic effects of silicon-doped graphene nanoflakes (GNF) on the reduction of CO_2 by H_2. Theoretical analyses were conducted using the TPSS/def2-SVP + D3BJ level of theory, and computations were performed using the ORCA 5.0.4 software suite. The findings revealed that Si-GNF exhibited lower activation energies and increased catalytic activity for CO_2 reduction compared to silicene, especially in the production of formic acid. Additionally, the conversion processes from formic acid to formaldehyde and formaldehyde to methanol were investigated, demonstrating the superior efficacy of Si-doped graphene over silicene.

In summary, graphene-based materials proved to be suitable supports for obtaining active, selective, and stable catalysts for CO_2 hydrogenation [244]. These materials can play a critical role in improving the selectivity and activity of catalysts by offering a versatile platform with tunable properties that can be tailored to specific catalytic needs. Their unique combination of stability, porosity, surface area, and electronic properties makes them a suitable choice in many catalytic applications. Additionally, in most of the studies reviewed (Table 6), it was verified that graphene-based supports can either match or improve the catalytic performance when compared to catalysts with conventional supports such as γ-Al_2O_3 and SiO_2. Moreover, rGO are widely used as a catalyst support thanks to their oxygen-containing functional groups, that enhance the stability of the active metal anchoring [251]. Gnp can also be used as a novel and promising candidate for heterogeneous catalysis due to their simple synthesis process, low costs, and the notable catalytic activity [249].

Despite the considerable potential of graphene-based material in catalysis, research in this area is still limited and lacks crucial in-depth investigations, notably in the case of methanation and rWGS reactions. Moreover, in the majority of studies (as represented in Table 6), GO and rGO are typically synthesized by using the modified Hummer's method, involving the use of harsh chemicals [30–32]. This approach causes significant challenges for the large-scale commercial synthesis of graphene-based catalysts, especially due to environmental, sustainability and health concerns. Moreover, the production cost depends on factors such as production methods, purity, and raw material availability; generally, graphene-based supports tend to be more expensive compared to alumina-based supports due to the currently higher cost of production and the relatively limited commercial availability of graphene materials. Graphene, being a relatively new and advanced material, often involves complex and expensive synthesis processes; additionally, the quality and purity of graphene can significantly affect its price[247,282–292]. These can act as a barrier for the transition toward the future of sustainable energy through the catalytic valorization of CO_2 by using graphene-based materials. On the contrary, MS approach in the synthesis of graphene-based materials, and consequently graphene-based catalysts, has the potential to substantially decrease both costs and environmental impacts, thereby facilitating the transition to large-scale production. However, it is essential to emphasize the need for further research and exploration in the field of molten salt and graphene-based catalysis to unlock its full potential for sustainable CO_2 valorization and the future of clean energy.

9. Conclusion

In this review, specific works on the use of molten salt for the synthesis of graphene by exfoliation of pristine graphite were discussed. The experiments were applied by using various setups, salts, atmospheres, temperatures, heating rates, and treatment times and the results prove that the properties of the obtained graphene are a function of applied conditions. Reported results indicate that the nature of used salt, high temperatures and high heating rates can lead to changes in the graphene structure with the formation of carbon nanocages, few layered graphene and arriving even to amorphous structures, thus allowing to tune process conditions for each identified application.

Among viable methods, both thermal and electrochemical exfoliation in molten salt could produce graphene-based materials from graphite. Both methods have their advantages and disadvantages, making it difficult to unambiguously determine which one is more promising for each application, including catalysis one. In fact, thermal exfoliation is a simple and cost-effective method that does not require special equipment, but the quality of the graphene produced is not as good as that produced by electrochemical exfoliation. On the other hand, electrochemical exfoliation is a more complex and expensive process, but it produces high-quality graphene. The choice between the two methods depends on the specific requirements and goal.

Several characterization techniques have been discussed. Among these techniques, Raman spectroscopy stands out for its capacity to quickly investigate both the structural and electronic characteristics of graphene. However, other methods such as AFM, SEM, TEM, XRD, and XPS provide complementary and important information regarding the morphology, crystal structure, surface chemistry, and the density of defects present in the material. It is essential to understand the complexities and limitations of each method to ensure accurate and comprehensive characterization of graphene-based materials.

Molten salt versatility could be even extended to a bottom-up approach for biomass pyrolysis offering advantages like improved efficiency and scalability, simplifying carbonization and activation into one single step, with potential benefits like no need for an inert atmosphere, and the possibility of salt recycling. Additionally, molten salt method can be used for the recycling of plastic waste such as PET into high-value graphene-based materials. This process not only mitigates the environmental impact of plastic pollution but also provides economic incentives by transforming waste into valuable resources.

Graphene-based material, with their exceptional properties has gained attention in catalysis and proved to be suitable supports for obtaining active, selective, and stable catalysts for CO_2 hydrogenation to high added-value compounds. They can offer a versatile platform with tunable properties that can be tailored to specific catalytic needs. However, the use of harsh chemicals in conventional synthesis of graphene derivatives causes challenges for large-scale production and can act as a barrier for the evolution toward the future of sustainable energy through the catalytic hydrogenation of CO_2. The top-down molten salt approach for the synthesis of graphene-like material shows the potential to overcome these challenges by offering a low-cost and environmental-friendly alternative. Nevertheless, further research is crucial to fully harness the potential of molten salt and graphene-based catalysis for sustainable CO_2 valorization for the development of clean energy.

Molten salt will play a crucial role in upgrading carbonaceous material coming from wastes, biomasses, biochar or even from turquoise H_2 production in an optic of net-zero emission and close carbon cycle; in fact, the development and use of advanced C-based materials will potentially increase the "storage time" delaying the emission of CO_2 in atmosphere. Accounting for the suitable choice of salts, furthermore, the use of concentrated brine arising from desalination processes could be even envisaged.

CRediT authorship contribution statement

Gabriella Garbarino: Writing – review & editing, Validation, Funding acquisition, Conceptualization. **Maria Paola Carpanese:** Writing – review & editing, Validation, Funding acquisition, Conceptualization. **Paola Riani:** Writing – review & editing, Validation, Funding acquisition, Conceptualization. **Elena Spennati:** Writing – review & editing, Validation. **Sina Ebrahim Atakoohi:** Writing – original draft.

Declaration of Competing Interest

The authors declare that they have no known competing financial interests or personal relationships that could have appeared to influence the work reported in this paper.

Data availability

No data was used for the research described in the article.

Acknowledgements

GG and ES acknowledge the Project funded under the National Recovery and Resilience Plan (NRRP), Mission 4 Component 2 Investment 1.3 - Call for tender No. 1561 of 11.10.2022 of Ministero dell'Università e della Ricerca (MUR); funded by the European Union – NextGenerationEU, PE0000021, "Network 4 Energy Sustainable Transition – NEST". PR and MPC acknowledge the PROMETH2eus project, RSH2A_000039 PNRR project of MASE Italian Ministry (missione 2 "Rivoluzione verde e transizione ecologica", componente 2 "Energia rinnovabile, idrogeno, rete e mobilità sostenibile", investimento 3.5 "Ricerca e sviluppo sull'idrogeno").

References

[1] K.S. Novoselov, A.K. Geim, S.V. Morozov, D. Jiang, Y. Zhang, S.V. Dubonos, I. V. Grigorieva, A.A. Firsov, Electric field in atomically thin carbon films, Science 306 (80) (2004) 666–669, https://doi.org/10.1126/SCIENCE.1102896/SUPPL_FILE/NOVOSELOV.SOM.PDF.
[2] A.K. Geim, K.S. Novoselov, The rise of graphene, Nanosci. Technol. A Collect. Rev. Nat. J. (2009) 11–19, https://doi.org/10.1142/9789814287005_0002.
[3] A.K. Geim, Graphene prehistory, Phys. Scr. (2012), https://doi.org/10.1088/0031-8949/2012/T146/014003.
[4] S. Navalon, A. Dhakshinamoorthy, M. Alvaro, H. Garcia, Carbocatalysis by graphene-based materials, Chem. Rev. 114 (2014) 6179–6212, https://doi.org/10.1021/cr4007347.
[5] A. Ambrosi, C.K. Chua, A. Bonanni, M. Pumera, Electrochemistry of graphene and related materials, Chem. Rev. 114 (2014) 7150–7188, https://doi.org/10.1021/cr500023c.
[6] A. Marinkas, F. Arena, J. Mitzel, G.M. Prinz, A. Heinzel, V. Peinecke, H. Natter, Graphene as catalyst support: the influences of carbon additives and catalyst preparation methods on the performance of PEM fuel cells, Carbon N. Y. 58 (2013) 139–150, https://doi.org/10.1016/j.carbon.2013.02.043.
[7] B. Chehroudi, Applications of graphene in fuel propellant combustion chehroudi 26 applications of graphene in fuel/propellant combustion, Graph. Sci. Handb. (2016).
[8] G. Centi, S. Perathoner, Opportunities and prospects in the chemical recycling of carbon dioxide to fuels, Catal. Today 148 (2009) 191–205, https://doi.org/10.1016/j.cattod.2009.07.075.
[9] S.K. Hoekman, A. Broch, C. Robbins, R. Purcell, CO2 recycling by reaction with renewably-generated hydrogen, Int. J. Greenh. Gas. Control 4 (2010) 44–50, https://doi.org/10.1016/j.ijggc.2009.09.012.
[10] G. Centi, S. Perathoner, Catalysis and sustainable (green) chemistry, Catal. Today 77 (2003) 287–297, https://doi.org/10.1016/S0920-5861(02)00374-7.
[11] G. Centi, S. Perathoner, Catalysis: Role and challenges for a sustainable energy, Top. Catal. 52 (2009) 948–961, https://doi.org/10.1007/s11244-009-9245-x.
[12] G. Garbarino, D. Bellotti, E. Finocchio, L. Magistri, G. Busca, Methanation of carbon dioxide on Ru/Al2O3: catalytic activity and infrared study, Catal. Today 277 (2016) 21–28, https://doi.org/10.1016/j.cattod.2015.12.010.
[13] A. Fasolini, E. Spennati, S. Ebrahim Atakoohi, M. Percivale, G. Busca, F. Basile, G. Garbarino, A study of CO2 hydrogenation over Ni-MgAlOx catalysts derived from hydrotalcite precursors, Catal. Today 423 (2023) 114271, https://doi.org/10.1016/j.cattod.2023.114271.
[14] M. Götz, J. Lefebvre, F. Mörs, A. McDaniel Koch, F. Graf, S. Bajohr, R. Reimert, T. Kolb, Renewable power-to-gas: a technological and economic review, Renew. Energy 85 (2016) 1371–1390, https://doi.org/10.1016/j.renene.2015.07.066.
[15] G. Lv, H. Wang, Y. Yang, T. Deng, C. Chen, Y. Zhu, X. Hou, Graphene oxide: a convenient metal-free carbocatalyst for facilitating aerobic oxidation of 5-hydroxymethylfurfural into 2, 5-diformylfuran, ACS Catal. 5 (2015) 5636–5646, https://doi.org/10.1021/acscatal.5b01446.
[16] C. Huang, C. Li, G. Shi, Graphene based catalysts, Energy Environ. Sci. 5 (2012) 8848–8868, https://doi.org/10.1039/c2ee22238h.
[17] X. Chen, Y. Chen, C. Song, P. Ji, N. Wang, W. Wang, L. Cui, Recent advances in supported metal catalysts and oxide catalysts for the reverse water-gas shift reaction, Front. Chem. 8 (2020) 1–21, https://doi.org/10.3389/fchem.2020.00709.
[18] Y. Yan, W.I. Shin, H. Chen, S.M. Lee, S. Manickam, S. Hanson, H. Zhao, E. Lester, T. Wu, C.H. Pang, A recent trend: application of graphene in catalysis, Carbon Lett. 31 (2021) 177–199, https://doi.org/10.1007/s42823-020-00200-7.
[19] C. Su, K.P. Loh, Carbocatalysts: graphene oxide and its derivatives, Acc. Chem. Res. 46 (2013) 2275–2285, https://doi.org/10.1021/ar300118v.
[20] H.Y. Zhuo, X. Zhang, J.X. Liang, Q. Yu, H. Xiao, J. Li, Theoretical understandings of graphene-based metal single-atom catalysts: stability and catalytic performance, Chem. Rev. 120 (2020) 12315–12341, https://doi.org/10.1021/ACS.CHEMREV.0C00818/ASSET/IMAGES/LARGE/CR0C00818_0015.JPEG.
[21] H. Su, Y.H. Hu, Recent advances in graphene-based materials for fuel cell applications, Energy Sci. Eng. 9 (2021) 958–983, https://doi.org/10.1002/ese3.833.
[22] IDTechEx, Graphene, 2D Materials and Carbon Nanotubes: Markets, Technologies and Opportunities 2017-2027: IDTechEx, IDTechEx (2017). ⟨http://www.idtechex.com/research/reports/graphene-2d-materials-and-carbon-nanotubes-markets-technologies-and-opportunities-2017-2027-000530.asp⟩ (accessed November 2, 2022).
[23] N. Kumar, R. Salehiyan, V. Chauke, O. Joseph Botlhoko, K. Setshedi, M. Scriba, M. Masukume, S. Sinha Ray, Top-down synthesis of graphene: a comprehensive review, FlatChem 27 (2021), https://doi.org/10.1016/j.flatc.2021.100224.
[24] Y. Xu, H. Cao, Y. Xue, B. Li, W. Cai, Liquid-phase exfoliation of graphene: an overview on exfoliation media, techniques, and challenges, Nanomaterials 8 (2018), https://doi.org/10.3390/nano8110942.
[25] J.R. Prekodravac, D.P. Kepić, J.C. Colmenares, D.A. Giannakoudakis, S. P. Jovanović, A comprehensive review on selected graphene synthesis methods: from electrochemical exfoliation through rapid thermal annealing towards biomass pyrolysis, J. Mater. Chem. C. 9 (2021) 6722–6748, https://doi.org/10.1039/d1tc01316e.
[26] Y. Yan, F.Z. Nashath, S. Chen, S. Manickam, S.S. Lim, H. Zhao, E. Lester, T. Wu, C. H. Pang, Synthesis of graphene: potential carbon precursors and approaches, Nanotechnol. Rev. 9 (2020) 1284–1314, https://doi.org/10.1515/ntrev-2020-0100.
[27] C.S. Giglio, O. Osazuwa, M. Kontopoulou, A. Docoslis, Achieving high yield of graphene nanoplatelets in poloxamer-assisted ultrasonication of graphite in water, J. Colloid Interface Sci. 539 (2019) 107–117, https://doi.org/10.1016/j.jcis.2018.12.033.
[28] W. Choi, I. Lahiri, R. Seelaboyina, Y.S. Kang, Synthesis of graphene and its applications: a review, Https://Doi.Org/10.1080/10408430903505036 35 (2010) 52–71, https://doi.org/10.1080/10408430903505036.
[29] D. Parviz, F. Irin, S.A. Shah, S. Das, C.B. Sweeney, M.J. Green, Challenges in liquid-phase exfoliation, processing, and assembly of pristine graphene, Adv. Mater. 28 (2016) 8796–8818, https://doi.org/10.1002/adma.201601889.
[30] S. Balasubramanyan, S. Sasidharan, R. Poovathinthodiyil, R.M. Ramakrishnan, B. N. Narayanan, Sucrose-mediated mechanical exfoliation of graphite: A green method for the large scale production of graphene and its application in catalytic reduction of 4-nitrophenol, N. J. Chem. 41 (2017) 11969–11978, https://doi.org/10.1039/c7nj01900a.
[31] B. Gürünlü, Ç. Taşdelen Yücedağ, M.R. Bayramoğlu, Green synthesis of graphene from graphite in molten salt medium, J. Nanomater. 2020 (2020), https://doi.org/10.1155/2020/7029601.
[32] D. Voiry, J. Yang, J. Kupferberg, R. Fullon, C. Lee, H.Y. Jeong, H.S. Shin, M. Chhowalla, High-quality graphene via microwave reduction of solution-exfoliated graphene oxide, Science 353 (80) (2016) 1413–1416, https://doi.org/10.1126/science.aah3398.
[33] H. Yu, B. Zhang, C. Bulin, R. Li, R. Xing, High-efficient synthesis of graphene oxide based on improved hummers method, Sci. Rep. 6 (2016), https://doi.org/10.1038/srep36143.
[34] Z. Benzait, P. Chen, L. Trabzon, Enhanced synthesis method of graphene oxide, Nanoscale Adv. 3 (2021) 223–230, https://doi.org/10.1039/d0na00706d.
[35] D.C. Marcano, D.V. Kosynkin, J.M. Berlin, A. Sinitskii, Z. Sun, A. Slesarev, L. B. Alemany, W. Lu, J.M. Tour, Improved synthesis of graphene oxide, ACS Nano 4 (2010) 4806–4814, https://doi.org/10.1021/nn1006368.
[36] F.M. Casallas Caicedo, E. Vera López, A. Agarwal, V. Drozd, A. Durygin, A. Franco Hernandez, C. Wang, Synthesis of graphene oxide from graphite by ball milling, Diam. Relat. Mater. 109 (2020), https://doi.org/10.1016/j.diamond.2020.108064.
[37] M. Yi, Z. Shen, A review on mechanical exfoliation for the scalable production of graphene, J. Mater. Chem. A 3 (2015) 11700–11715, https://doi.org/10.1039/c5ta00252d.
[38] S. Lim, J.H. Han, H.W. Kang, J.U. Lee, W. Lee, Preparation of electrochemically exfoliated graphene sheets using DC switching voltages, Carbon Lett. 30 (2020) 409–416, https://doi.org/10.1007/s42823-019-00110-3.

[39] Ö. Güler, M. Tekeli, M. Taşkın, S.H. Güler, I.S. Yahia, The production of graphene by direct liquid phase exfoliation of graphite at moderate sonication power by using low boiling liquid media: The effect of liquid media on yield and optimization, Ceram. Int. 47 (2021) 521–533, https://doi.org/10.1016/j.ceramint.2020.08.159.
[40] L. Zhu, X. Zhao, Y. Li, X. Yu, C. Li, Q. Zhang, High-quality production of graphene by liquid-phase exfoliation of expanded graphite, Mater. Chem. Phys. 137 (2013) 984–990, https://doi.org/10.1016/j.matchemphys.2012.11.012.
[41] R. Narayan, S.O. Kim, Surfactant mediated liquid phase exfoliation of graphene, Nano Converg. 2 (2015), https://doi.org/10.1186/s40580-015-0050-x.
[42] E. Ruse, M. Larboni, A. Lavi, M. Pyrikov, Y. Leibovitch, A. Ohayon-Lavi, L. Vradman, O. Regev, Molten salt in-situ exfoliation of graphite to graphene nanoplatelets applied for energy storage, Carbon N. Y. 176 (2021) 168–177, https://doi.org/10.1016/j.carbon.2021.01.133.
[43] A. Griffin, K. Nisi, J. Pepper, A. Harvey, B.M. Szydłowska, J.N. Coleman, C. Backes, Effect of surfactant choice and concentration on the dimensions and yield of liquid-phase-exfoliated nanosheets, Chem. Mater. 32 (2020) 2852–2862, https://doi.org/10.1021/acs.chemmater.9b04684.
[44] Y. Hernandez, V. Nicolosi, M. Lotya, F.M. Blighe, Z. Sun, S. De, I.T. McGovern, B. Holland, M. Byrne, Y.K. Gun'ko, J.J. Boland, P. Niraj, G. Duesberg, S. Krishnamurthy, R. Goodhue, J. Hutchison, V. Scardaci, A.C. Ferrari, J. N. Coleman, High-yield production of graphene by liquid-phase exfoliation of graphite, Nat. Nanotechnol. 3 (2008) 563–568, https://doi.org/10.1038/nnano.2008.215.
[45] V.A. Yolshina, L.A. Yolshina, Electrochemical synthesis of graphene in molten salts, Russ. Metall. 2021 (2021) 206–212, https://doi.org/10.1134/S0036029521020051.
[46] J. Yang, K. Du, L. Hu, D. Wang, Scalable fabrication of carbon nanomaterials by electrochemical dual-electrode exfoliation of graphite in hydroxide molten salt, Ind. Eng. Chem. Res. 59 (2020) 10010–10017, https://doi.org/10.1021/acs.iecr.0c01430.
[47] M. Zhang, L. Liu, T. He, X. Ju, P. Chen, Molten salt assisted pyrolysis approach for the synthesis of nitrogen-rich microporous carbon nanosheets and its application as gas capture sorbent, Microporous Mesoporous Mater. 300 (2020), https://doi.org/10.1016/J.MICROMESO.2020.110177.
[48] M.T. Alshamkhani, P. Lahijani, K.T. Lee, A.R. Mohamed, Electrochemical exfoliation of graphene using dual graphite electrodes by switching voltage and green molten salt electrolyte, Ceram. Int. 48 (2022) 22534–22546, https://doi.org/10.1016/j.ceramint.2022.04.268.
[49] A. Rezaei, A.R. Kamali, Green production of carbon nanomaterials in molten salts, mechanisms and applications, Diam. Relat. Mater. 83 (2018) 146–161, https://doi.org/10.1016/j.diamond.2018.02.003.
[50] X. Liu, N. Fechler, M. Antonietti, Salt melt synthesis of ceramics, semiconductors and carbon nanostructures, Chem. Soc. Rev. 42 (2013) 8237–8265, https://doi.org/10.1039/c3cs60159e.
[51] X. Xiao, H. Jia, S. Pervaiz, D. Wen, Molten salt/metal foam/graphene nanoparticle phase change composites for thermal energy storage, ACS Appl. Nano Mater. 3 (2020) 5240–5251, https://doi.org/10.1021/acsanm.0c00648.
[52] Z. He, L. Gao, X. Wang, B. Zhang, W. Qi, J. Song, X. He, C. Zhang, H. Tang, H. Xia, X. Zhou, Improvement of stacking order in graphite by molten fluoride salt infiltration, Carbon N. Y. 72 (2014) 304–311, https://doi.org/10.1016/j.carbon.2014.02.010.
[53] J. Wang, S. Feng, Y. Yang, H. Tang, X. Liu, H. Xia, Y. Wang, X. Zhou, Effect of tensile strength on the microstructure of graphite impregnated with salt revealed by in situ synchrotron-based two-dimensional x-ray diffraction, ACS Omega 4 (2019) 4304–4311, https://doi.org/10.1021/acsomega.8b03329.
[54] S. Mrozowski, Electric resistivity of interstitial compounds of graphite, J. Chem. Phys. 21 (1953) 492–495, https://doi.org/10.1063/1.1698933.
[55] N. Díez, A.B. Fuertes, M. Sevilla, Molten salt strategies towards carbon materials for energy storage and conversion, Energy Storage Mater. 38 (2021) 50–69, https://doi.org/10.1016/j.ensm.2021.02.048.
[56] Z. Pang, G. Li, X. Xiong, L. Ji, Q. Xu, X. Zou, X. Lu, Molten salt synthesis of porous carbon and its application in supercapacitors: a review, J. Energy Chem. 61 (2021) 622–640, https://doi.org/10.1016/j.jechem.2021.02.020.
[57] Q. Sun, S. Zhu, Z. Shen, Y. Liu, C. Wu, L. Kang, Y. Yang, Molten-salt assisted synthesis of two-dimensional materials and energy storage application, Mater. Today Chem. 29 (2023), https://doi.org/10.1016/j.mtchem.2023.101419.
[58] S. Sharma, A.S. Ivanov, C.J. Margulis, A brief guide to the structure of high-temperature molten salts and key aspects making them different from their low-temperature relatives, the ionic liquids, J. Phys. Chem. B 125 (2021) 6359–6372, https://doi.org/10.1021/acs.jpcb.1c01065.
[59] R. Roper, M. Harkema, P. Sabharwall, C. Riddle, B. Chisholm, B. Day, P. Marotta, Molten salt for advanced energy applications: a review, Ann. Nucl. Energy 169 (2022) 108924, https://doi.org/10.1016/j.anucene.2021.108924.
[60] Y. He, B. Song, X. Jing, Y. Zhou, H. Chang, W. Yang, Z. Huang, Low-carbon hydrogen production via molten salt methane pyrolysis with chemical looping combustion: emission reduction potential and techno-economic assessment, Fuel Process. Technol. 247 (2023), https://doi.org/10.1016/j.fuproc.2023.107778.
[61] C. Palmer, M. Tarazkar, M.J. Gordon, H. Metiu, E.W. McFarland, Methane pyrolysis in low-cost, alkali-halide molten salts at high temperatures, Sustain. Energy Fuels 5 (2021) 6107–6123, https://doi.org/10.1039/D1SE01408K.
[62] D. Kang, C. Palmer, D. Mannini, N. Rahimi, M.J. Gordon, H. Metiu, E. W. McFarland, Catalytic methane pyrolysis in molten alkali chloride salts containing iron, ACS Catal. 10 (2020) 7032–7042, https://doi.org/10.1021/acscatal.0c01262.
[63] J.R. Selman, Molten salt fuel cells: diversity and convergence, cycles and recycling, Int. J. Hydrog. Energy 46 (2021) 15078–15094, https://doi.org/10.1016/j.ijhydene.2020.05.197.
[64] I.L. Egun, H. He, D. Hu, G.Z. Chen, Molten salt carbonization and activation of biomass to functional biocarbon, Adv. Sustain. Syst. 6 (2022), https://doi.org/10.1002/adsu.202200294.
[65] H.S. Nygård, E. Olsen, Review of thermal processing of biomass and waste in molten salts for production of renewable fuels and chemicals, Int. J. Low. Carbon Technol. 7 (2012) 318–324, https://doi.org/10.1093/ijlct/ctr045.
[66] M. Bi, S.J. Hwang, K.R. Morris, Mechanism of eutectic formation upon compaction and its effects on tablet properties, Thermochim. Acta 404 (2003) 213–226, https://doi.org/10.1016/S0040-6031(03)00185-0.
[67] M.H. Zainal-Abidin, M. Hayyan, G.C. Ngoh, W.F. Wong, C.Y. Looi, Emerging frontiers of deep eutectic solvents in drug discovery and drug delivery systems, J. Control. Release 316 (2019) 168–195, https://doi.org/10.1016/j.jconrel.2019.09.019.
[68] S. Cherukuvada, A. Nangia, Eutectics as improved pharmaceutical materials: design, properties and characterization, Chem. Commun. 50 (2014) 906–923, https://doi.org/10.1039/c3cc47521b.
[69] W.F. Smith, J. Hashemi, Foundations of Materials Science and Engineering, MsGraw-Hill Companies, Inc, New York NY, 2006, p. 10020. ISBN 72953586 (2010) 1032.
[70] T. Ozawa, M. Kamimoto, Chapter 7 Energy storage, Handb. Therm. Anal. Calorim. 2 (2003) 307–348, https://doi.org/10.1016/S1573-4374(03)80011-0.
[71] I.A. Tahiri, Matiullah, M.S. Subhani, Molten Ba(OH)2·8H2O as an etchant for CR-39 detector, Radiat. Meas. 37 (2003) 205–210, https://doi.org/10.1016/S1350-4487(03)00030-1.
[72] P. Li, C.L. Chan, Q. Hao, P.A. Deymier, K. Muralidharan, D.F. Gervasio, M. Momayez, S. Jeter, A.S. Teja, A.M. Kannan, Halide and oxy-halide eutectic systems for high performance high temperature heat transfer fluids, SunShot Conc. Sol. Power Progr. Rev. 2013 (2013) 85–86.
[73] A. Lavi, M. Pyrikov, A. Ohayon-Lavi, R. Tadmor, G. Shachar-Michaely, Y. Leibovitch, E. Ruse, L. Vradman, O. Regev, Total exfoliation of graphite in molten salts, Phys. Chem. Chem. Phys. (2022) 2618–2628, https://doi.org/10.1039/d2cp01613c.
[74] A. Bianco, H.M. Cheng, T. Enoki, Y. Gogotsi, R.H. Hurt, N. Koratkar, T. Kyotani, M. Monthioux, C.R. Park, J.M.D. Tascon, J. Zhang, All in the graphene family - a recommended nomenclature for two-dimensional carbon materials, Carbon N. Y. 65 (2013) 1–6, https://doi.org/10.1016/j.carbon.2013.08.038.
[75] S. Roscher, R. Hoffmann, O. Ambacher, Determination of the graphene–graphite ratio of graphene powder by Raman 2D band symmetry analysis, Anal. Methods 11 (2019) 1224–1228, https://doi.org/10.1039/C8AY02619J.
[76] M. Mandal, A. Maitra, T. Das, C.K. Das, Graphene and related two-dimensional materials, Graph. Mater. Fundam. Emerg. Appl. (2015) 1–23, https://doi.org/10.1002/9781119131816.ch1.
[77] B. Partoens, F.M. Peeters, From graphene to graphite: electronic structure around the K point, Phys. Rev. B - Condens. Matter Mater. Phys. 74 (2006) 1–11, https://doi.org/10.1103/PhysRevB.74.075404.
[78] V. Palermo, I.A. Kinloch, S. Ligi, N.M. Pugno, Nanoscale mechanics of graphene and graphene oxide in composites: a scientific and technological perspective, Adv. Mater. 28 (2016) 6232–6238, https://doi.org/10.1002/adma.201505469.
[79] A.C. Ferrari, D.M. Basko, Raman spectroscopy as a versatile tool for studying the properties of graphene, Nat. Nanotechnol. 8 (2013) 235–246, https://doi.org/10.1038/nnano.2013.46.
[80] I. Childres, L.A. Jauregui, W. Park, H. Caoa, Y.P. Chena, Raman spectroscopy of graphene and related materials, N. Dev. Phot. Mater. Res. (2013) 403–418.
[81] M. Wall, The Raman spectroscopy of graphene and the determination of layer thickness, Thermo Sci. 5 (2011).
[82] M.S. Dresselhaus, A. Jorio, R. Saito, Characterizing graphene, graphite, and carbon nanotubes by Raman spectroscopy, Annu. Rev. Condens. Matter Phys. 1 (2010) 89–108, https://doi.org/10.1146/annurev-conmatphys-070909-103919.
[83] Y. Hao, Y. Wang, L. Wang, Z. Ni, Z. Wang, R. Wang, C.K. Koo, Z. Shen, J.T. L. Thong, Probing layer number and stacking order of few-layer graphene by Raman Spectroscopy, Small 6 (2010) 195–200, https://doi.org/10.1002/smll.200901173.
[84] A.C. Ferrari, Raman spectroscopy of graphene and graphite: disorder, electron-phonon coupling, doping and nonadiabatic effects, Solid State Commun. 143 (2007) 47–57, https://doi.org/10.1016/j.ssc.2007.03.052.
[85] J.Bin Wu, M.L. Lin, X. Cong, H.N. Liu, P.H. Tan, Raman spectroscopy of graphene-based materials and its applications in related devices, Chem. Soc. Rev. 47 (2018) 1822–1873, https://doi.org/10.1039/c6cs00915h.
[86] D. Graf, F. Molitor, K. Ensslin, C. Stampfer, A. Jungen, C. Hierold, L. Wirtz, Spatially resolved raman spectroscopy of single- and few-layer graphene, Nano Lett. 7 (2007) 238–242, https://doi.org/10.1021/nl061702a.
[87] W. Sheng, T. Shi, B. Sun, X. Tan, T. Jiang, G. Liao, Three dimensional metal film catalyst assisted etching of silicon, Tech. Proc. 2013 NSTI Nanotechnol, 2013, Conf. Expo. NSTI Nanotech 2 (2013) 427–430.
[88] F. TUINSTRA, J.L. KOENIG, Raman spectrum of graphite, J. Chem. Phys. 53 (2003) 1126, https://doi.org/10.1063/1.1674108.
[89] Å. Björkman, Thermische Klärschlammbehandlung, Schweiz. Z. F. üR. Hydrol. 31 (1969) 632–645, https://doi.org/10.1007/BF02543692.
[90] V. Scardaci, G. Compagnini, Raman spectroscopy investigation of graphene oxide reduction by laser scribing, C 7 (2021) 48, https://doi.org/10.3390/c7020048.
[91] T. Palaniselvam, H.B. Aiyappa, S. Kurungot, An efficient oxygen reduction electrocatalyst from graphene by simultaneously generating pores and nitrogen

doped active sites, J. Mater. Chem. 22 (2012) 23799–23805, https://doi.org/10.1039/c2jm35128e.
[92] V. Kumar, A. Kumar, D.J. Lee, S.S. Park, Estimation of number of graphene layers using different methods: a focused review, Materials 14 (2021), https://doi.org/10.3390/ma14164590.
[93] C.N.R. Rao, A.K. Sood, K.S. Subrahmanyam, A. Govindaraj, Graphene: the new two-dimensional nanomaterial, Angew. Chem. - Int. Ed. 48 (2009) 7752–7777, https://doi.org/10.1002/anie.200901678.
[94] J. Epp, X-ray diffraction (XRD) techniques for materials characterization, Mater. Charact. Using Nondestruct. Eval. Methods (2016) 81–124, https://doi.org/10.1016/B978-0-08-100040-3.00004-3.
[95] A.R. Bushroa, R.G. Rahbari, H.H. Masjuki, M.R. Muhamad, Approximation of crystallite size and microstrain via XRD line broadening analysis in TiSiN thin films, Vacuum 86 (2012) 1107–1112, https://doi.org/10.1016/j.vacuum.2011.10.011.
[96] M. Mauro, V. Cipolletti, M. Galimberti, P. Longo, G. Guerra, Chemically reduced graphite oxide with improved shape anisotropy, J. Phys. Chem. C. 116 (2012) 24809–24813, https://doi.org/10.1021/jp307112k.
[97] M. Hu, Z. Yao, X. Wang, Characterization techniques for graphene-based materials in catalysis, AIMS Mater. Sci. 4 (2017) 755–788, https://doi.org/10.3934/matersci.2017.3.755.
[98] F.T. Johra, J.W. Lee, W.G. Jung, Facile and safe graphene preparation on solution based platform, J. Ind. Eng. Chem. 20 (2014) 2883–2887, https://doi.org/10.1016/j.jiec.2013.11.022.
[99] G. Gao, D. Liu, S. Tang, C. Huang, M. He, Y. Guo, X. Sun, B. Gao, Heat-initiated chemical functionalization of graphene, Sci. Rep. 6 (1) (2016) 8, https://doi.org/10.1038/srep20034.
[100] F. Buchner, K. Forster-Tonigold, M. Bozorgchenani, A. Gross, R.J. Behm, Interaction of a self-assembled ionic liquid layer with graphite(0001): a combined experimental and theoretical study, J. Phys. Chem. Lett. 7 (2016) 226–233, https://doi.org/10.1021/acs.jpclett.5b02449.
[101] R.J. Zaldivar, P.M. Adams, J. Nokes, H.I. Kim, Surface functionalization of graphenelike materials by carbon monoxide atmospheric plasma treatment for improved wetting without structural degradation, J. Vac. Sci. Technol. B, Nanotechnol. Microelectron. Mater. Process. Meas. Phenom. 30 (2012), https://doi.org/10.1116/1.3695337.
[102] A. Kolmakov, D.A. Dikin, L.J. Cote, J. Huang, M.K. Abyaneh, M. Amati, L. Gregoratti, S. Günther, M. Kiskinova, Graphene oxide windows for in situ environmental cell photoelectron spectroscopy, Nat. Nanotechnol. 6 (2011) 651–657, https://doi.org/10.1038/nnano.2011.130.
[103] B.F. Spencer, S. Maniyarasu, B.P. Reed, D.J.H. Cant, R. Ahumada-Lazo, A. G. Thomas, C.A. Muryn, M. Maschek, S.K. Eriksson, T. Wiell, T.L. Lee, S. Tougaard, A.G. Shard, W.R. Flavell, Inelastic background modelling applied to hard X-ray photoelectron spectroscopy of deeply buried layers: a comparison of synchrotron and lab-based (9.25 keV) measurements, Appl. Surf. Sci. 541 (2021) 148635, https://doi.org/10.1016/j.apsusc.2020.148635.
[104] A.R. Kamali, D.J. Fray, Molten salt corrosion of graphite as a possible way to make carbon nanostructures, Carbon N. Y. 56 (2013) 121–131, https://doi.org/10.1016/j.carbon.2012.12.076.
[105] X. Liang, J. Guo, S. Liang, C. Hong, Y. Zhao, Synthesis of soluble graphene nanosheets from graphite fluoride in low-temperature molten hydroxides, Mater. Lett. 135 (2014) 92–95, https://doi.org/10.1016/j.matlet.2014.07.119.
[106] G. Xin, Y. Wang, J. Zang, S. Jia, P. Tian, S. Zhou, Temperature tuned carbon morphologies derived from flexible graphite sheets in KNO3 molten salt, Carbon N. Y. 98 (2016) 221–224, https://doi.org/10.1016/J.CARBON.2015.11.016.
[107] W. Gumlich, P.W. Selwood, 1956, , Partially 79838–841.
[108] X. Cheng, H. Liu, H. Yuan, H. Peng, C. Tang, J. Huang, Q. Zhang, A perspective on sustainable energy materials for lithium batteries, SusMat 1 (2021) 38–50, https://doi.org/10.1002/sus2.4.
[109] J. Xu, H.R. Thomas, R.W. Francis, K.R. Lum, J. Wang, B. Liang, A review of processes and technologies for the recycling of lithium-ion secondary batteries, J. Power Sources 177 (2008) 512–527, https://doi.org/10.1016/j.jpowsour.2007.11.074.
[110] B. Shahzad, M. Tanveer, W. Hassan, A.N. Shah, S.A. Anjum, S.A. Cheema, I. Ali, Lithium toxicity in plants: Reasons, mechanisms and remediation possibilities – a review, Plant Physiol. Biochem. 107 (2016) 104–115, https://doi.org/10.1016/j.plaphy.2016.05.034.
[111] 2021, The Role of Critical Minerals in Clean Energy Transitions, OECD, Paris10.1787/f262b91c-en..
[112] A. Hirsch, The era of carbon allotropes, Nat. Mater. 9 (2010) 868–871, https://doi.org/10.1038/nmat2885.
[113] T. Jalalabadi, J. Wu, B. Moghtaderi, N. Sharma, J. Allen, A new approach to turbostratic carbon production via thermal salt-assisted treatment of graphite, Fuel 348 (2023) 128489, https://doi.org/10.1016/j.fuel.2023.128489.
[114] P. Ruz, S. Banerjee, M. Pandey, V. Sudarsan, P.U. Sastry, R.J. Kshirsagar, Structural evolution of turbostratic carbon: implications in H2 storage, Solid State Sci. 62 (2016) 105–111, https://doi.org/10.1016/j.solidstatesciences.2016.10.017.
[115] D. Yu, W. Cao, H. Wu, J. Zhao, Ionic radius scale of establishing synthesis factor of ionic mass and electricity, Acta Phys. - Chim. Sin. 23 (2007) 683–687, https://doi.org/10.1016/S1872-1508(07)60043-6.
[116] H.D.B. Jenkins, K.P. Thakur, Reappraisal of thermochemical radii for complex ions, J. Chem. Educ. 56 (1979) 576–577, https://doi.org/10.1021/ed056p576.
[117] H.K. Roobottom, H.D.B. Jenkins, J. Passmore, L. Glasser, Thermochemical radii of complex ions, J. Chem. Educ. 76 (1999) 1570–1572, https://doi.org/10.1021/ed076p1570.
[118] E.A. Belenkov, Formation of graphite structure in carbon crystallites, Inorg. Mater. 37 (2001) 928–934, https://doi.org/10.1023/A:1011601915600.
[119] A.A. Pirzado, F. Le Normand, T. Romero, S. Paszkiewicz, V. Papaefthimiou, D. Ihiawakrim, I. Janowska, Few-layer graphene from mechanical exfoliation of graphite-based materials: structure-dependent characteristics, ChemEngineering 3 (2019) 1–10, https://doi.org/10.3390/chemengineering3020037.
[120] A. Gutiérrez-Cruz, A.R. Ruiz-Hernández, J.F. Vega-Clemente, D.G. Luna-Gazcón, J. Campos-Delgado, A review of top-down and bottom-up synthesis methods for the production of graphene, graphene oxide and reduced graphene oxide, J. Mater. Sci. 57 (2022) 14543–14578, https://doi.org/10.1007/s10853-022-07514-z.
[121] M. Rahm, R. Hoffmann, N.W. Ashcroft, Atomic and Ionic Radii of Elements 1–96, Chem. - A Eur. J. 22 (2016) 14625–14632, https://doi.org/10.1002/chem.201602949.
[122] S. Komaba, T. Hasegawa, M. Dahbi, K. Kubota, Potassium intercalation into graphite to realize high-voltage/high-power potassium-ion batteries and potassium-ion capacitors, Electrochem. Commun. 60 (2015) 172–175, https://doi.org/10.1016/j.elecom.2015.09.002.
[123] Y. Zhu, S. Murali, W. Cai, X. Li, J.W. Suk, J.R. Potts, R.S. Ruoff, Graphene and graphene oxide: synthesis, properties, and applications, Adv. Mater. 22 (2010) 3906–3924, https://doi.org/10.1002/adma.201001068.
[124] S. Wang, C. Wang, X. Ji, Towards understanding the salt-intercalation exfoliation of graphite into graphene, RSC Adv. 7 (2017) 52252–52260, https://doi.org/10.1039/c7ra07489a.
[125] Frederic LantelmeHenri Groult, Book - MOLTEN SALTS CHEMISTRY FROM LAB TO APPLICATION, Elsevier 4 (2557) 88–100.
[126] M. Parrinello, A. Rahman, Study of an F center in molten KCl, J. Chem. Phys. 80 (1998) 860, https://doi.org/10.1063/1.446740.
[127] H. Bloom, Chemistry of molten salts, Solid State Commun. 5 (1967) vii, https://doi.org/10.1016/0038-1098(67)90824-1.
[128] Y. Marcus, Ionic Liquid Properties: From Molten Salts to RTILs, Springer International Publishing, 2016, https://doi.org/10.1007/978-3-319-30313-0.
[129] F. Bresme, J. Alejandre, Cavities in ionic liquids, J. Chem. Phys. 118 (2003) 4134–4139, https://doi.org/10.1063/1.1540090.
[130] R. Takagi, H. Ohno, K. Furukawa, Structure of molten KCl, J. Chem. Soc. Faraday Trans. 1 Phys. Chem. Condens. Phases (1979) 1477–1486, https://doi.org/10.1039/F19797501477.
[131] H.A. Levy, P.A. Agron, M.A. Bredig, M.D. Danford, X-ray and neutron diffraction studies of molten alkali halides, Ann. N. Y. Acad. Sci. 79 (1960) 762–780, https://doi.org/10.1111/j.1749-6632.1960.tb42753.x.
[132] X. Song, S. Li, S. Liu, Y. Fan, J. He, J. Song, Coordination states of metal ions in molten salts and their characterization methods, J. Chem. Soc. Faraday Trans. 1 Phys. Chem. Condens. Phases 30 (2023) 1261–1277, https://doi.org/10.1007/s12613-023-2608-7.
[133] M. Shimoji, Interaction in molten salt mixtures, Discuss. Faraday Soc. 32 (1961) 128–137, https://doi.org/10.1039/DF9613200128.
[134] G. Yoon, D.H. Seo, K. Ku, J. Kim, S. Jeon, K. Kang, Factors affecting the exfoliation of graphite intercalation compounds for graphene synthesis, Chem. Mater. 27 (2015) 2067–2073, https://doi.org/10.1021/cm504511b.
[135] J.N. Israelachvili, Intermolecular and surface forces, Intermol. Surf. Forces- 2nd Ed. 53 (1992) 710.
[136] M. Cai, D. Thorpe, D.H. Adamson, H.C. Schniepp, Methods of graphite exfoliation, J. Mater. Chem. 22 (2012) 24992–25002, https://doi.org/10.1039/c2jm34517j.
[137] S.A. Safran, Interfacial Tension, Stat. Thermodyn. Surf. Interfaces, Membr. (2018) 55–74, https://doi.org/10.1201/9780429497131-2/INTERFACIAL-TENSION-SAMUEL-SAFRAN.
[138] A.L. Sutton, V.C. Howard, The role of porosity in the accommodation of thermal expansion in graphite, J. Nucl. Mater. 7 (1962) 58–71, https://doi.org/10.1016/0022-3115(62)90194-0.
[139] K. Wen, J. Marrow, B. Marsden, Microcracks in nuclear graphite and highly oriented pyrolytic graphite (HOPG), J. Nucl. Mater. 381 (2008) 199–203, https://doi.org/10.1016/j.jnucmat.2008.07.012.
[140] P.J. Hacker, G.B. Neighbour, B. McEnaney, Coefficient of thermal expansion of nuclear graphite with increasing thermal oxidation, J. Phys. D. Appl. Phys. 33 (2000) 991–998, https://doi.org/10.1088/0022-3727/33/8/316.
[141] Y. Wei, Z. Sun, Liquid-phase exfoliation of graphite for mass production of pristine few-layer graphene, Curr. Opin. Colloid Interface Sci. 20 (2015) 311–321, https://doi.org/10.1016/j.cocis.2015.10.010.
[142] K.S. Suslick, D.J. Flannigan, Inside a collapsing bubble: sonoluminescence and the conditions during cavitation, Annu. Rev. Phys. Chem. 59 (2008) 659–683, https://doi.org/10.1146/annurev.physchem.59.032607.093739.
[143] K. Krishnamoorthy, G.S. Kim, S.J. Kim, Graphene nanosheets: ultrasound assisted synthesis and characterization, Ultrason. Sonochem. 20 (2013) 644–649, https://doi.org/10.1016/j.ultsonch.2012.09.007.
[144] B.Z. Jang, A. Zhamu, Processing of nanographene platelets (NGPs) and NGP nanocomposites: a review, J. Mater. Sci. 43 (2008) 5092–5101, https://doi.org/10.1007/s10853-008-2755-2.
[145] K.R. Paton, E. Varrla, C. Backes, R.J. Smith, U. Khan, A. O'Neill, C. Boland, M. Lotya, O.M. Istrate, P. King, T. Higgins, S. Barwich, P. May, P. Puczkarski, I. Ahmed, M. Moebius, H. Pettersson, E. Long, J. Coelho, S.E. O'Brien, E. K. McGuire, B.M. Sanchez, G.S. Duesberg, N. McEvoy, T.J. Pennycook, C. Downing, A. Crossley, V. Nicolosi, J.N. Coleman, Scalable production of large quantities of defect-free few-layer graphene by shear exfoliation in liquids, Nat. Mater. 13 (2014) 624–630, https://doi.org/10.1038/nmat3944.
[146] A.R. Kamali, Green production of carbon nanomaterials in molten salts and applications, 2020. https://doi.org/10.1007/978-981-15-2373-1.

[147] P. Yu, S.E. Lowe, G.P. Simon, Y.L. Zhong, Electrochemical exfoliation of graphite and production of functional graphene, Curr. Opin. Colloid Interface Sci. 20 (2015) 329–338, https://doi.org/10.1016/j.cocis.2015.10.007.

[148] J.M. Munuera, J.I. Paredes, M. Enterría, A. Pagán, S. Villar-Rodil, M.F.R. Pereira, J.I. Martins, J.L. Figueiredo, J.L. Cenis, A. Martínez-Alonso, J.M.D. Tascón, Electrochemical exfoliation of graphite in aqueous sodium halide electrolytes toward low oxygen content graphene for energy and environmental applications, ACS Appl. Mater. Interfaces 9 (2017) 24085–24099, https://doi.org/10.1021/acsami.7b04802.

[149] C.T.J. Low, F.C. Walsh, M.H. Chakrabarti, M.A. Hashim, M.A. Hussain, Electrochemical approaches to the production of graphene flakes and their potential applications, Carbon N. Y. 54 (2013) 1–21, https://doi.org/10.1016/j.carbon.2012.11.030.

[150] W.K. Hsu, P.J.F. Harris, M. Terrones, H.W. Kroto, D.R.M. Walton, Condensed-phase nanotubes, Nature 377 (1995) 687, https://doi.org/10.1038/377687a0.

[151] W.K. Hsu, M. Terrones, J.P. Hare, H. Terrones, H.W. Kroto, D.R.M. Walton, Electrolytic formation of carbon nanostructures, Chem. Phys. Lett. 262 (1996) 161–166, https://doi.org/10.1016/0009-2614(96)01041-X.

[152] G.Z. Chen, X. Fan, A. Luget, M.S.P. Shaffer, D.J. Fray, A.H. Windle, Electrolytic conversion of graphite to carbon nanotubes in fused salts, J. Electroanal. Chem. 446 (1998) 1–6, https://doi.org/10.1016/S0022-0728(97)00552-4.

[153] Q. Xu, C. Schwandt, G.Z. Chen, D.J. Fray, Electrochemical investigation of lithium intercalation into graphite from molten lithium chloride, J. Electroanal. Chem. 530 (2002) 16–22, https://doi.org/10.1016/S0022-0728(02)00998-1.

[154] L. Labiadh, A.R. Kamali, 3D graphene nanoedges as efficient dye adsorbents with ultra-high thermal regeneration performance, Appl. Surf. Sci. 490 (2019) 383–394, https://doi.org/10.1016/j.apsusc.2019.06.081.

[155] A. Rezaei, B. Kamali, A.R. Kamali, Correlation between morphological, structural and electrical properties of graphite and exfoliated graphene nanostructures, Meas. J. Int. Meas. Confed. 150 (2020), https://doi.org/10.1016/j.measurement.2019.107087.

[156] J. Sytchev, G. Kaptay, Influence of current density on the erosion of a graphite cathode and electrolytic formation of carbon nanotubes in molten NaCl and LiCl, Electrochim. Acta 54 (2009) 6725–6731, https://doi.org/10.1016/j.electacta.2009.06.055.

[157] C. Schwandt, A.T. Dimitrov, D.J. Fray, The preparation of nano-structured carbon materials by electrolysis of molten lithium chloride at graphite electrodes, J. Electroanal. Chem. 647 (2010) 150–158, https://doi.org/10.1016/j.jelechem.2010.06.008.

[158] A.R. Kamali, D.J. Fray, Large-scale preparation of graphene by high temperature insertion of hydrogen into graphite, Nanoscale 7 (2015) 11310–11320, https://doi.org/10.1039/c5nr01132a.

[159] A.R. Kamali, C. Schwandt, D. J. Fray, Effect of the graphite electrode material on the characteristics of molten salt electrolytically produced carbon nanomaterials, Mater. Charact. 62 (2011) 987–994, https://doi.org/10.1016/j.matchar.2011.06.010.

[160] H. Huang, Y. Xia, X. Tao, J. Du, J. Fang, Y. Gan, W. Zhang, Highly efficient electrolytic exfoliation of graphite into graphene sheets based on Li ions intercalation-expansion-microexplosion mechanism, J. Mater. Chem. 22 (2012) 10452–10456, https://doi.org/10.1039/c2jm00092j.

[161] A.R. Kamali, D.J. Fray, Towards large scale preparation of carbon nanostructures in molten LiCl, Carbon N. Y. 77 (2014) 835–845, https://doi.org/10.1016/j.carbon.2014.05.089.

[162] A.M. Abdelkader, Electrochemical synthesis of highly corrugated graphene sheets for high performance supercapacitors, J. Mater. Chem. A 3 (2015) 8519–8525, https://doi.org/10.1039/c5ta00545k.

[163] A.R. Kamali, Eco-friendly production of high quality low cost graphene and its application in lithium ion batteries, Green. Chem. 18 (2016) 1952–1964, https://doi.org/10.1039/c5gc02455b.

[164] A.R. Kamali, J. Feighan, D.J. Fray, Towards large scale preparation of graphene in molten salts and its use in the fabrication of highly toughened alumina ceramics, Faraday Discuss. 190 (2016) 451–470, https://doi.org/10.1039/c6fd00005c.

[165] J. Zhu, Y. Xiang, J. Zhao, H. Wang, Y. Li, B. Zheng, H. He, Z. Zhang, J. Huang, Y. Yang, Insights into the local structure, microstructure and ionic conductivity of silicon doped NASICON-type solid electrolyte Li1.3Al0.3Ti1.7P3O12, Energy Storage Mater. 44 (2022) 190–196, https://doi.org/10.1016/j.ensm.2021.10.003.

[166] N.Q. Minh, B.J. Welch, The cathodic reduction of HCl dissolved in LiCl+KCl+ZnCl2 melts, J. Electroanal. Chem. 92 (1978) 179–189, https://doi.org/10.1016/S0022-0728(78)80177-6.

[167] N.Q. Minh, B.J. Welch, Stoichiometry and mechanism of the cathodic reduction process for HCl dissolved in LiCl-KCl eutectic, Aust. J. Chem. 28 (1975) 2579–2585, https://doi.org/10.1071/CH9752579.

[168] N.Q. Minh, B.J. Welch, The reduction of HCl dissolved in LiCl-KCl eutectic, Aust. J. Chem. 28 (1975) 965–973, https://doi.org/10.1071/CH9750965.

[169] Lithium shortages: threat or opportunity? - Mining Technology, (n.d.). ⟨https://www.mining-technology.com/features/lithium-price-challenges/⟩ (accessed December 11, 2022).

[170] A.R. Kamali, Scalable fabrication of highly conductive 3D graphene by electrochemical exfoliation of graphite in molten NaCl under Ar/H2 atmosphere, J. Ind. Eng. Chem. 52 (2017) 18–27, https://doi.org/10.1016/j.jiec.2017.03.013.

[171] S. Wamucci, Lettuce price in US - 2022 prices and charts, (n.d.). ⟨https://www.selinawamucii.com/insights/prices/united-states-of-america/table-salt/⟩ (accessed December 14, 2022).

[172] Lithium Statistics and Information | U.S. Geological Survey, Miner. Commod. Summ. (2018). ⟨https://www.usgs.gov/centers/national-minerals-information-center/lithium-statistics-and-information⟩ (accessed December 14, 2022).

[173] A.R. Kamali, D.J. Fray, C. Schwandt, Thermokinetic characteristics of lithium chloride, J. Therm. Anal. Calorim. 104 (2011) 619–626, https://doi.org/10.1007/s10973-010-1045-9.

[174] Y. Zhang, Y. Xu, J. Zhu, L. Li, X. Du, X. Sun, Electrochemically exfoliated high-yield graphene in ambient temperature molten salts and its application for flexible solid-state supercapacitors, Elsevier Ltd (2018), https://doi.org/10.1016/j.carbon.2017.11.002.

[175] A.M. Abdelkader, C. Vallés, A.J. Cooper, I.A. Kinloch, R.A.W. Dryfe, Alkali reduction of graphene oxide in molten halide salts: production of corrugated graphene derivatives for high-performance supercapacitors, ACS Nano 8 (2014) 11225–11233, https://doi.org/10.1021/nn505700x.

[176] J. Wang, B. Ding, X. Hao, Y. Xu, Y. Wang, L. Shen, H. Dou, X. Zhang, A modified molten-salt method to prepare graphene electrode with high capacitance and low self-discharge rate, Carbon N. Y. 102 (2016) 255–261, https://doi.org/10.1016/j.carbon.2016.02.047.

[177] W. Ai, J. Jiang, J. Zhu, Z. Fan, Y. Wang, H. Zhang, W. Huang, T. Yu, Supramolecular polymerization promoted in situ fabrication of nitrogen-doped porous graphene sheets as anode materials for Li-ion batteries, Adv. Energy Mater. 5 (2015) 1–8, https://doi.org/10.1002/aenm.201500559.

[178] J. Luo, J. Kim, J. Huang, Material processing of chemically modified graphene: some challenges and solutions, Acc. Chem. Res. 46 (2013) 2225–2234, https://doi.org/10.1021/ar300180n.

[179] Y. Zhou, Q. Bao, L.A.L. Tang, Y. Zhong, K.P. Loh, Hydrothermal dehydration for the "green" reduction of exfoliated graphene oxide to graphene and demonstration of tunable optical limiting properties, Chem. Mater. 21 (2009) 2950–2956, https://doi.org/10.1021/cm9006603.

[180] S. Pei, H.M. Cheng, The reduction of graphene oxide, Carbon N. Y. 50 (2012) 3210–3228, https://doi.org/10.1016/j.carbon.2011.11.010.

[181] H.C. Schniepp, J.L. Li, M.J. McAllister, H. Sai, M. Herrera-Alonson, D. H. Adamson, R.K. Prud'homme, R. Car, D.A. Seville, I.A. Aksay, Functionalized single graphene sheets derived from splitting graphite oxide, J. Phys. Chem. B 110 (2006) 8535–8539, https://doi.org/10.1021/jp060936f.

[182] X. Wang, L. Zhi, K. Müllen, Transparent, conductive graphene electrodes for dye-sensitized solar cells, Nano Lett. 8 (2008) 323–327, https://doi.org/10.1021/nl072838r.

[183] S. Stankovich, D.A. Dikin, R.D. Piner, K.A. Kohlhaas, A. Kleinhammes, Y. Jia, Y. Wu, S.B.T. Nguyen, R.S. Ruoff, Synthesis of graphene-based nanosheets via chemical reduction of exfoliated graphite oxide, Carbon N. Y. 45 (2007) 1558–1565, https://doi.org/10.1016/j.carbon.2007.02.034.

[184] Y. Si, E.T. Samulski, Synthesis of water soluble graphene, Nano Lett. 8 (2008) 1679–1682, https://doi.org/10.1021/nl080604h.

[185] D. Rauchteilchen, D. Praxis, Die Reduktion yon G r a p h i t o x y d mit S c h w e f e l w a s s e r s t o f f., 2 (1934) 149–151.

[186] J. Zhao, S. Pei, W. Ren, L. Gao, H.M. Cheng, Efficient preparation of large-area graphene oxide sheets for transparent conductive films, ACS Nano 4 (2010) 5245–5252, https://doi.org/10.1021/nn1015506.

[187] I.K. Moon, J. Lee, R.S. Ruoff, H. Lee, Reduced graphene oxide by chemical graphitization, Nat. Commun. 1 (2010), https://doi.org/10.1038/ncomms1067.

[188] W. Guoxiu, Y. Juan, P. Jinsoo, G. Xinglong, W. Bei, L. Hao, Y. Jane, Facile synthesis and characterization of graphene nanosheets, J. Phys. Chem. C. 112 (2008) 8192–8195, https://doi.org/10.1021/jp710931h.

[189] S. Stankovich, D.A. Dikin, G.H.B. Dommett, K.M. Kohlhaas, E.J. Zimney, E. A. Stach, R.D. Piner, S.B.T. Nguyen, R.S. Ruoff, Graphene-based composite materials, Nature 442 (2006) 282–286, https://doi.org/10.1038/nature04969.

[190] L. Zhao, X. Liu, C. Wan, X. Ye, F. Wu, Soluble Graphene Nanosheets from Recycled Graphite of Spent Lithium Ion Batteries, J. Mater. Eng. Perform. 27 (2018) 875–880, https://doi.org/10.1007/s11665-018-3156-6.

[191] V.S. Dilimon, S. Sampath, Electrochemical preparation of few layer-graphene nanosheets via reduction of oriented exfoliated graphene oxide thin films in acetamide-urea-ammonium nitrate melt under ambient conditions, Thin Solid Films 519 (2011) 2323–2327, https://doi.org/10.1016/j.tsf.2010.11.019.

[192] X. Liu, C. Giordano, M. Antonietti, A facile molten-salt route to graphene synthesis 8 (1) (2013), https://doi.org/10.1002/smll.201300812.

[193] Y. Shen, Research advancement in molten salt-mediated thermochemical upcycling of biomass waste, (2023) 2087–2108. https://doi.org/10.1039/d2gc04872h.

[194] B. Li, J. Tang, X. Xie, J. Wei, D. Xu, L. Shi, K. Ding, S. Zhang, X. Hu, S. Zhang, D. Liu, Char structure evolution during molten salt pyrolysis of biomass: effect of temperature, Fuel 331 (2023), https://doi.org/10.1016/j.fuel.2022.125747.

[195] S.E. Atakoohi, E. Spennati, A.A. Casazza, P. Riani, G. Garbarino, Investigating the effect of operational variables on the yield, characterization, and properties of end-of-life olive stone biomass pyrolysis products, Molecules 28 (2023), https://doi.org/10.3390/molecules28186516.

[196] D. Lee, H. Nam, M. Won Seo, S. Hoon Lee, D. Tokmurzin, S. Wang, Y.K. Park, Recent progress in the catalytic thermochemical conversion process of biomass for biofuels, Chem. Eng. J. 447 (2022), https://doi.org/10.1016/j.cej.2022.137501.

[197] C. Zhou, J. Zhang, Y. Pei, K. Tian, X. Zhang, X. Yan, Bioresource Technology Molten salt strategy to activate biochar for enhancing biohydrogen production, Bioresour. Technol. 385 (2023) 129466, https://doi.org/10.1016/j.biortech.2023.129466.

[198] B. Li, M. Li, X. Xie, C. Li, D. Liu, Pyrolysis of rice husk in molten lithium chloride: Biochar structure evolution and CO 2 adsorption, J. Energy Inst. 113 (2024) 101526, https://doi.org/10.1016/j.joei.2024.101526.
[199] P. Li, H. Xie, Y. Liu, J. Wang, Y. Xie, W. Hu, T. Xie, Y. Wang, Y. Zhang, Molten salt and air induced nitrogen-containing graphitic hierarchical porous biocarbon nanosheets derived from kitchen waste hydrolysis residue for energy storage, J. Power Sources 439 (2019), https://doi.org/10.1016/j.jpowsour.2019.227096.
[200] L. Yang, J. Qiu, Y. Wang, S. Guo, Y. Feng, D. Dong, J. Yao, Molten salt synthesis of hierarchical porous carbon from wood sawdust for supercapacitors, J. Electroanal. Chem. 856 (2020) 113673, https://doi.org/10.1016/j.jelechem.2019.113673.
[201] J. Yang, H. Xu, H. Chen, F. Meng, H. Zu, P. Zhu, Z. Yang, M. Li, H. Li, Removal of flue gas mercury by porous carbons derived from one-pot carbonization and activation of wood sawdust in a molten salt medium, J. Hazard. Mater. 424 (2022), https://doi.org/10.1016/j.jhazmat.2021.127336.
[202] X. Du, Z. Lin, Y. Zhang, P. Li, Microstructural tailoring of porous few-layer graphene-like biochar from kitchen waste hydrolysis residue in molten carbonate medium: Structural evolution and conductive additive-free supercapacitor application, Sci. Total Environ, Sci. Total Environ. 871 (2023) 162045, https://doi.org/10.1016/j.scitotenv.2023.162045.
[203] X. Qi, H. Zhang, C. Li, D. Chen, C. Sun, Z. Yang, A simple and recyclable molten-salt route to prepare superthin biocarbon sheets based on the high water-absorbent agaric for efficient lithium storage, Carbon N. Y. 157 (2020) 286–294, https://doi.org/10.1016/j.carbon.2019.10.050.
[204] D. Zeng, Y. Dou, M. Li, M. Zhou, H. Li, K. Jiang, F. Yang, J. Peng, Wool fiber-derived nitrogen-doped porous carbon prepared from molten salt carbonization method for supercapacitor application, J. Mater. Sci. 53 (2018) 8372–8384, https://doi.org/10.1007/s10853-018-2035-8.
[205] H. Zhang, Z. Zhang, J.Di Luo, X.T. Qi, J. Yu, J.X. Cai, Z.Y. Yang, Molten-salt-assisted synthesis of hierarchical porous MnO@biocarbon composites as promising electrode materials for supercapacitors and lithium-ion batteries, ChemSusChem 12 (2019) 283–290, https://doi.org/10.1002/cssc.201802245.
[206] P. Tian, Y. Wang, S. Jia, H. Gao, S. Zhou, H. Xu, S. Song, J. Zang, Frying" milk powder by molten salt to prepare nitrogen-doped hierarchical porous carbon for high performance supercapacitor, J. Alloy. Compd. 806 (2019) 650–659, https://doi.org/10.1016/j.jallcom.2019.07.266.
[207] X. Liu, C. Yu, Z. Chen, F. Xu, W. Liao, W. Zhong, Biomass peach gum-derived heteroatom-doped porous carbon via in situ molten salt activation for high-performance supercapacitors, Energy Fuels 35 (2021) 19801–19810, https://doi.org/10.1021/acs.energyfuels.1c03064.
[208] C. Wang, D. Wu, H. Wang, Z. Gao, F. Xu, K. Jiang, A green and scalable route to yield porous carbon sheets from biomass for supercapacitors with high capacity, J. Mater. Chem. A 6 (2018) 1244–1254, https://doi.org/10.1039/c7ta07579k.
[209] W. Lei, B. Yang, Y. Sun, L. Xiao, D. Tang, K. Chen, J. Sun, J. Ke, Y. Zhuang, Self-sacrificial template synthesis of heteroatom doped porous biochar for enhanced electrochemical energy storage, J. Power Sources 488 (2021), https://doi.org/10.1016/j.jpowsour.2021.229455.
[210] S. Liu, J. Xu, J. Zhu, Y. Chang, H. Wang, Z. Liu, Y. Xu, C. Zhang, T. Liu, Leaf-inspired interwoven carbon nanosheet/nanotube homostructures for supercapacitors with high energy and power densities, J. Mater. Chem. A 5 (2017) 19997–20004, https://doi.org/10.1039/c7ta04952h.
[211] Y. Xie, W. Hu, X. Wang, W. Tong, P. Li, H. Zhou, Y. Wang, Y. Zhang, Molten salt induced nitrogen-doped biochar nanosheets as highly efficient peroxymonosulfate catalyst for organic pollutant degradation, Environ. Pollut. 260 (2020), https://doi.org/10.1016/j.envpol.2020.114053.
[212] Y. Liu, H. Tan, Z. Tan, X. Cheng, Rice husk derived capacitive carbon prepared by one-step molten salt carbonization for supercapacitors, J. Energy Storage 55 (2022), https://doi.org/10.1016/j.est.2022.105437.
[213] Z. Guo, X. Kong, X. Wu, W. Xing, J. Zhou, Y. Zhao, S. Zhuo, Heteroatom-doped hierarchical porous carbon via molten-salt method for supercapacitors, Electrochim. Acta 360 (2020), https://doi.org/10.1016/j.electacta.2020.137022.
[214] F. Liu, J. Ding, G. Zhao, Q. Zhao, K. Wang, G. Wang, Q. Gao, Catalytic pyrolysis of lotus leaves for producing nitrogen self-doping layered graphitic biochar: performance and mechanism for peroxydisulfate activation, Chemosphere 302 (2022) 134868, https://doi.org/10.1016/j.chemosphere.2022.134868.
[215] H. Shang, Y. Lu, F. Zhao, C. Chao, B. Zhang, H. Zhang, Preparing high surface area porous carbon from biomass by carbonization in a molten salt medium, RSC Adv. 5 (2015) 75728–75734, https://doi.org/10.1039/c5ra12406a.
[216] D. Liu, L. Yang, J. Wu, B. Li, Molten salt shielded preparation of rice straw biochars doped by copper sulfide for elemental mercury capture, J. Energy Inst. 102 (2022) 176–183, https://doi.org/10.1016/j.joei.2022.03.005.
[217] M. Yin, X. Bai, D. Wu, F. Li, K. Jiang, N. Ma, Z. Chen, X. Zhang, L. Fang, Sulfur-functional group tunning on biochar through sodium thiosulfate modified molten salt process for efficient heavy metal adsorption, Chem. Eng. J. 433 (2022), https://doi.org/10.1016/j.cej.2021.134441.
[218] D. Wu, J. Hu, C. Zhu, J. Zhang, H. Jing, C. Hao, Y. Shi, Salt melt synthesis of Chlorella-derived nitrogen-doped porous carbon with atomically dispersed CoN4 sites for efficient oxygen reduction reaction, J. Colloid Interface Sci. 586 (2021) 498–504, https://doi.org/10.1016/j.jcis.2020.10.115.
[219] P. Wang, G. Zhang, W. Chen, Q. Chen, H. Jiao, L. Liu, X. Wang, X. Deng, Molten salt template synthesis of hierarchical porous nitrogen-containing activated carbon derived from chitosan for CO2capture, ACS Omega 5 (2020) 23460–23467, https://doi.org/10.1021/acsomega.0c03497.
[220] B. Lu, J. Zhou, Y. Song, H. Wang, W. Xiao, D. Wang, Molten-salt treatment of waste biomass for preparation of carbon with enhanced capacitive properties and electrocatalytic activity towards oxygen reduction, Faraday Discuss. 190 (2016) 147–159, https://doi.org/10.1039/c5fd00215j.
[221] Y. Cheng, B. Li, Y. Huang, Y. Wang, J. Chen, D. Wei, Y. Feng, D. Jia, Y. Zhou, Molten salt synthesis of nitrogen and oxygen enriched hierarchically porous carbons derived from biomass via rapid microwave carbonization for high voltage supercapacitors, Appl. Surf. Sci. 439 (2018) 712–723, https://doi.org/10.1016/j.apsusc.2018.01.006.
[222] X. Deng, B. Zhao, L. Zhu, Z. Shao, Molten salt synthesis of nitrogen-doped carbon with hierarchical pore structures for use as high-performance electrodes in supercapacitors, Carbon N. Y. 93 (2015) 48–58, https://doi.org/10.1016/j.carbon.2015.05.031.
[223] B. Lu, L. Hu, H. Yin, X. Mao, W. Xiao, D. Wang, Preparation and application of capacitive carbon from bamboo shells by one step molten carbonates carbonization, Int. J. Hydrog. Energy 41 (2016) 18713–18720, https://doi.org/10.1016/j.ijhydene.2016.05.083.
[224] C. Wang, D. Wu, H. Wang, Z. Gao, F. Xu, K. Jiang, Nitrogen-doped two-dimensional porous carbon sheets derived from clover biomass for high performance supercapacitors, J. Power Sources 363 (2017) 375–383, https://doi.org/10.1016/j.jpowsour.2017.07.097.
[225] B. Lu, L. Hu, H. Yin, W. Xiao, D. Wang, One-step molten salt carbonization (MSC) of firwood biomass for capacitive carbon, RSC Adv. 6 (2016) 106485–106490, https://doi.org/10.1039/c6ra22191b.
[226] X. Lu, Y. Zhang, H. Zhong, L. Yang, X. Xu, H. Liu, C. Yuan, Molten-salt strategy for fabrication of hierarchical porous N-doped carbon nanosheets towards high-performance supercapacitors, Mater. Chem. Phys. 230 (2019) 178–186, https://doi.org/10.1016/j.matchemphys.2019.03.051.
[227] D. Wang, C. Wen, B. Zhang, G. Zhu, W. Wen, Q. Liu, Sustainable eutectic mixture strategy of molten salts for preparing biochar with interconnected pore structure from algal residue and its performance in aqueous supercapacitor, J. Energy Storage 69 (2023) 107935, https://doi.org/10.1016/j.est.2023.107935.
[228] A.R. Kamali, J. Yang, Q. Sun, Applied surface science molten salt conversion of polyethylene terephthalate waste into graphene nanostructures with high surface area and ultra-high electrical conductivity, Appl. Surf. Sci. 476 (2019) 539–551, https://doi.org/10.1016/j.apsusc.2019.01.119.
[229] Roland Geyer, Jenna R. Jambeck, Law K. Lavender, Production, use, and fate of all plastics ever made, Sci. Adv. 3 (2017).
[230] A. Naji, M. Nuri, A.D. Vethaak, Microplastics contamination in molluscs from the northern part of the Persian Gulf, Environ. Pollut. 235 (2018) 113–120, https://doi.org/10.1016/j.envpol.2017.12.046.
[231] M. Carbery, W. O'Connor, T. Palanisami, Trophic transfer of microplastics and mixed contaminants in the marine food web and implications for human health, Environ. Int. 115 (2018) 400–409, https://doi.org/10.1016/j.envint.2018.03.007.
[232] T.S. Gallowaya, C.N. Lewisa, Marine microplastics spell big problems for future generations, Proc. Natl. Acad. Sci. U. S. A. 113 (2016) 2331–2333, https://doi.org/10.1073/pnas.1600715113.
[233] L. Van Cauwenberghe, C.R. Janssen, Microplastics in bivalves cultured for human consumption, Environ. Pollut. 193 (2014) 65–70, https://doi.org/10.1016/j.envpol.2014.06.010.
[234] K. Chikaoui, M. Izerrouken, M. Djebara, M. Abdesselam, Polyethylene terephthalate degradation under reactor neutron irradiation, Radiat. Phys. Chem. 130 (2017) 431–435, https://doi.org/10.1016/j.radphyschem.2016.10.002.
[235] A.A. Aboul-Enein, A.E. Awadallah, Production of nanostructured carbon materials using Fe–Mo/MgO catalysts via mild catalytic pyrolysis of polyethylene waste, Chem. Eng. J. 354 (2018) 802–816, https://doi.org/10.1016/j.cej.2018.08.046.
[236] K. Zhang, Z. Huang, M. Yang, M. Liu, Y. Zhou, J. Zhan, Y. Zhou, Recent progress in melt pyrolysis: Fabrication and applications of high-value carbon materials from abundant sources, SusMat 3 (2023) 558–580, https://doi.org/10.1002/sus2.157.
[237] G.E. Bertolini, J. Fontaine, Value recovery from plastics waste by pyrolysis in molten salts, Conserv. Recycl. 10 (1987) 331–343, https://doi.org/10.1016/0361-3658(87)90064-6.
[238] A.R. Kamali, J. Yang, Q. Sun, Molten salt conversion of polyethylene terephthalate waste into graphene nanostructures with high surface area and ultra-high electrical conductivity, Appl. Surf. Sci. 476 (2019) 539–551, https://doi.org/10.1016/j.apsusc.2019.01.119.
[239] A.R. Kamali, J. Yang, Effect of molten salts on the structure, morphology and electrical conductivity of PET-derived carbon nanostructures, Polym. Degrad. Stab. 177 (2020) 109184, https://doi.org/10.1016/j.polymdegradstab.2020.109184.
[240] M. Götz, J. Lefebvre, F. Mörs, A. McDaniel Koch, F. Graf, S. Bajohr, R. Reimert, T. Kolb, Renewable power-to-gas: a technological and economic review, Renew. Energy 85 (2016) 1371–1390, https://doi.org/10.1016/j.renene.2015.07.066.
[241] G. Busca, E. Spennati, P. Riani, G. Garbarino, Looking for an optimal composition of nickel-based catalysts for CO2 methanation, Energies 16 (2023), https://doi.org/10.3390/en16145304.
[242] P. Riani, E. Spennati, M.V. Garcia, V.S. Escribano, G. Busca, G. Garbarino, Ni/Al2O3 catalysts for CO2 methanation: Effect of silica and nickel loading, Int. J. Hydrog. Energy 48 (2023) 24976–24995, https://doi.org/10.1016/j.ijhydene.2023.01.002.
[243] G. Garbarino, P. Kowalik, P. Riani, K. Antoniak-Jurak, P. Pieta, A. Lewalska-Graczyk, W. Lisowski, R. Nowakowski, G. Busca, I.S. Pieta, Improvement of Ni/Al2O3catalysts for low-temperature CO2methanation by vanadium and calcium oxide addition, Ind. Eng. Chem. Res. 60 (2021) 6554–6564, https://doi.org/10.1021/acs.iecr.0c05556.

[244] M. Mihet, M. Dan, M.D. Lazar, CO2 hydrogenation catalyzed by graphene-based materials, Page 3367 27 (2022) 3367, Molecules Vol. 27 (2022), https://doi.org/10.3390/MOLECULES27113367.
[245] G. Busca, E. Spennati, P. Riani, G. Garbarino, Mechanistic and compositional aspects of industrial catalysts for selective CO2 hydrogenation processes, Catalysts 14 (2024) 95, https://doi.org/10.3390/catal14020095.
[246] C. Huang, C. Li, G. Shi, Graphene based catalysts, Energy Environ. Sci. 5 (2012) 8848–8868, https://doi.org/10.1039/c2ee22238h.
[247] Y. Yan, W.I. Shin, H. Chen, S.M. Lee, S. Manickam, S. Hanson, H. Zhao, E. Lester, T. Wu, C.H. Pang, A recent trend: application of graphene in catalysis, Carbon Lett. 31 (2021) 177–199, https://doi.org/10.1007/s42823-020-00200-7.
[248] D.R. Dreyer, S. Park, C.W. Bielawski, R.S. Ruoff, The chemistry of graphene oxide, Chem. Soc. Rev. 39 (2010) 228–240, https://doi.org/10.1039/b917103g.
[249] L. Zhong, T.H.M. Pham, Y. Ko, A. Züttel, Graphene nanoplatelets promoted CoO-based catalyst for low temperature CO2 methanation reaction, Front. Chem. Eng. 5 (2023) 1–9, https://doi.org/10.3389/fceng.2023.1160254.
[250] L.T.M. Nguyen, H. Park, M. Banu, J.Y. Kim, D.H. Youn, G. Magesh, W.Y. Kim, J. S. Lee, Catalytic CO2 hydrogenation to formic acid over carbon nanotube-graphene supported PdNi alloy catalysts, RSC Adv. 5 (2015) 105560–105566, https://doi.org/10.1039/c5ra21017h.
[251] F. Hu, S. Tong, K. Lu, C.M. Chen, F.Y. Su, J. Zhou, Z.H. Lu, X. Wang, G. Feng, R. Zhang, Reduced graphene oxide supported Ni-Ce catalysts for CO2 methanation: the support and ceria promotion effects, J. CO2 Util. 34 (2019) 676–687, https://doi.org/10.1016/J.JCOU.2019.08.020.
[252] N.Diyan Mohd Ridzuan, M.Shima Shaharun, K.Mun Lee, I. Ud Din, P. Puspitasari, Influence of nickel loading on reduced graphene oxide-based nickel catalysts for the hydrogenation of carbon dioxide to methane, Catalysts 10 (2020), https://doi.org/10.3390/catal10050471.
[253] H. Zhong, M. Iguchi, M. Chatterjee, T. Ishizaka, M. Kitta, Q. Xu, H. Kawanami, Interconversion between CO2 and HCOOH under basic conditions catalyzed by PdAu nanoparticles supported by amine-functionalized reduced graphene oxide as a dual catalyst, ACS Catal. 8 (2018) 5355–5362, https://doi.org/10.1021/acscatal.8b00294.
[254] J. Sirijaraensre, J. Limtrakul, Hydrogenation of CO 2 to formic acid over a Cu-embedded graphene: a DFT study, Appl. Surf. Sci. 364 (2016) 241–248, https://doi.org/10.1016/j.apsusc.2015.12.117.
[255] W.E. Vallejo Narváez, S. Fomine, Silicon-doped graphene as a catalyst for hydrogenation of carbon dioxide: a molecular simulation study, ChemistrySelect 9 (2024), https://doi.org/10.1002/slct.202303649.
[256] F. Hu, X. Chen, Z. Tu, Z.H. Lu, G. Feng, R. Zhang, Graphene aerogel supported Ni for CO2hydrogenation to methane, Ind. Eng. Chem. Res. 60 (2021) 12235–12243, https://doi.org/10.1021/acs.iecr.1c01953.
[257] T.R. Mignoli, T.L.R. Hewer, R.M.B. Alves, M. Schmal, Reduced graphene oxide (rGO) as new support of cobalt/lanthanum oxide for the water gas shift reaction (WGSR), Appl. Catal. A Gen. 635 (2022) 118553, https://doi.org/10.1016/j.apcata.2022.118553.
[258] J. Wu, C. Wen, X. Zou, J. Jimenez, J. Sun, Y. Xia, M.T. Fonseca Rodrigues, S. Vinod, J. Zhong, N. Chopra, I.N. Odeh, G. Ding, J. Lauterbach, P.M. Ajayan, Carbon dioxide hydrogenation over a metal-free carbon-based catalyst, ACS Catal. 7 (2017) 4497–4503, https://doi.org/10.1021/ACSCATAL.7B00729/ASSET/IMAGES/LARGE/CS-2017-007293_0005.JPEG.
[259] A. Mohanty, C.D. Viet, A.C. Roger, A. Adam, D. Mertz, W. Baaziz, I. Janowska, Structural impact of carbon nanofibers/few-layer-graphene substrate decorated with Ni for CO2 methanation via inductive heating, Appl. Catal. B Environ. 298 (2021) 120589, https://doi.org/10.1016/J.APCATB.2021.120589.
[260] L. Peng, B. Jurca, A. Primo, A. Gordillo, V.I. Parvulescu, H. García, Co-Fe clusters supported on N-doped graphitic carbon as highly selective catalysts for reverse water gas shift reaction, ACS Sustain. Chem. Eng. 9 (2021) 9264–9272, https://doi.org/10.1021/acssuschemeng.1c01401.
[261] C. Wang, P. Zhai, Z. Zhang, Y. Zhou, J. Zhang, H. Zhang, Z. Shi, R.P.S. Han, F. Huang, D. Ma, Nickel catalyst stabilization via graphene encapsulation for enhanced methanation reaction, J. Catal. 334 (2016) 42–51, https://doi.org/10.1016/j.jcat.2015.10.004.
[262] W. Malik, J.P. Victoria Tafoya, S. Doszczeczko, A.B. Jorge Sobrido, V.K. Skoulou, A.N. Boa, Q. Zhang, T. Ramirez Reina, R. Volpe, Synthesis of a graphene-encapsulated Fe3C/Fe catalyst supported on sporopollenin exine capsules and its use for the reverse water-gas shift reaction, ACS Sustain. Chem. Eng. 11 (2023) 15795–15807, https://doi.org/10.1021/acssuschemeng.3c00495.
[263] T. Witoon, T. Numpilai, T. Phongamwong, W. Donphai, C. Boonyuen, C. Warakulwit, M. Chareonpanich, J. Limtrakul, Enhanced activity, selectivity and stability of a CuO-ZnO-ZrO2 catalyst by adding graphene oxide for CO2 hydrogenation to methanol, Chem. Eng. J. 334 (2018) 1781–1791, https://doi.org/10.1016/j.cej.2017.11.117.
[264] D. Méndez-Mateos, V.L. Barrio, J.M. Requies, M. Gil-Calvo, Graphene-based versus alumina supports on CO2 methanation using lanthanum-promoted nickel catalysts, Environ. Sci. Pollut. Res. (2023), https://doi.org/10.1007/s11356-023-26324-7.
[265] Z.J. Liu, X.J. Tang, S. Xu, X.L. Wang, Synthesis and catalytic performance of graphene modified CuO-ZnO-Al2O3 for CO2 hydrogenation to methanol, J. Nanomater. 2014 (2014), https://doi.org/10.1155/2014/690514.
[266] Y. Tano, M.S. Ahmad, Y. Watase, T. Tsugawa, S. Takase, Y. Inomata, K. Hatakeyama, S. Ida, Q. Armando, Y. Shimizu, T. Kida, Enhancement of formic acid formation by nitrogen-doped graphene oxide nanosheets decorated with Sn nanoparticles in electrochemical CO2 reduction, Sustain. Energy Fuels 7 (2023) 3964–3971, https://doi.org/10.1039/d3se00781b.
[267] V. Deerattrakul, P. Puengampholsrisook, W. Limphirat, P. Kongkachuichay, Characterization of supported Cu-Zn/graphene aerogel catalyst for direct CO2 hydrogenation to methanol: effect of hydrothermal temperature on graphene aerogel synthesis, Catal. Today 314 (2018) 154–163, https://doi.org/10.1016/j.cattod.2017.12.010.
[268] V. Deerattrakul, N. Yigit, G. Rupprechter, P. Kongkachuichay, The roles of nitrogen species on graphene aerogel supported Cu-Zn as efficient catalysts for CO2 hydrogenation to methanol, Appl. Catal. A Gen. 580 (2019) 46–52, https://doi.org/10.1016/j.apcata.2019.04.030.
[269] F. He, N. Niu, F. Qu, S. Wei, Y. Chen, S. Gai, P. Gao, Y. Wang, P. Yang, Synthesis of three-dimensional reduced graphene oxide layer supported cobalt nanocrystals and their high catalytic activity in F-T CO2 hydrogenation, Nanoscale 5 (2013) 8507–8516, https://doi.org/10.1039/c3nr03038e.
[270] X. San, X. Gong, Y. Hu, Y. Hu, G. Wang, J. Qi, D. Meng, Q. Jin, Highly dispersed Cu/graphene nanocatalyst guided by MOF structure: application to methanol synthesis from CO2 hydrogenation, ChemistrySelect 6 (2021) 6115–6118, https://doi.org/10.1002/slct.202101179.
[271] T. Wu, J. Lin, Y. Cheng, J. Tian, S. Wang, S. Xie, Y. Pei, S. Yan, M. Qiao, H. Xu, B. Zong, Porous graphene-confined Fe-K as highly efficient catalyst for CO2 direct hydrogenation to light olefins, ACS Appl. Mater. Interfaces 10 (2018) 23439–23443, https://doi.org/10.1021/acsami.8b05411.
[272] V. Deerattrakul, P. Dittanet, M. Sawangphruk, P. Kongkachuichay, CO2 hydrogenation to methanol using Cu-Zn catalyst supported on reduced graphene oxide nanosheets, J. CO2 Util. 16 (2016) 104–113, https://doi.org/10.1016/j.jcou.2016.07.002.
[273] Y.J. Fan, S.F. Wu, A graphene-supported copper-based catalyst for the hydrogenation of carbon dioxide to form methanol, J. CO2 Util. 16 (2016) 150–156, https://doi.org/10.1016/j.jcou.2016.07.001.
[274] S. Wang, T. Wu, J. Lin, J. Tian, Y. Ji, Y. Pei, S. Yan, M. Qiao, H. Xu, B. Zong, FeK on 3D graphene-zeolite tandem catalyst with high efficiency and versatility in direct CO2 conversion to aromatics, ACS Sustain. Chem. Eng. 7 (2019) 17825–17833, https://doi.org/10.1021/acssuschemeng.9b04328.
[275] Q. Ma, M. Geng, J. Zhang, X. Zhang, T.S. Zhao, Enhanced catalytic performance for CO2 hydrogenation to methanol over N-doped graphene incorporated Cu-ZnO-Al2O3 catalysts, ChemistrySelect 4 (2019) 78–83, https://doi.org/10.1002/slct.201803186.
[276] S. Alinia, M. Masoumi, A. Haghtalab, M. Otadi, F. Yaripour, Enhanced Fischer-Tropsch synthesis performance using graphene nanosheets-supported cobalt-ruthenium nanocatalysts: comparative study with γ -alumina and carbon nanotubes supports, Arab. J. Chem. 17 (2024) 105503, https://doi.org/10.1016/j.arabjc.2023.105503.
[277] C. Wang, Y. Fang, G. Liang, X. Lv, H. Duan, Y. Li, D. Chen, M. Long, Mechanistic study of Cu-Ni bimetallic catalysts supported by graphene derivatives for hydrogenation of CO2to methanol, J. CO2 Util. 49 (2021), https://doi.org/10.1016/j.jcou.2021.101542.
[278] S. Karimi, A. Tavasoli, Y. Mortazavi, A. Karimi, Applied catalysis a: general cobalt supported on graphene – a promising novel Fischer – Tropsch synthesis catalyst, Appl. Catal. A, Gen. 499 (2015) 188–196, https://doi.org/10.1016/j.apcata.2015.04.024.
[279] J. Chang, Y. Zhang, X. Lu, Y. Yao, X. Liu, D. Hildebrandt, Applied Catalysis A, general insight into the role of Co 2 C supported on reduced graphene oxide in Fischer-Tropsch synthesis and ethene hydroformylation, Appl. Catal. A, Gen. 614 (2021) 118050, https://doi.org/10.1016/j.apcata.2021.118050.
[280] A. Aghababai, Z. Pournuroz, Preparation of cobalt-ruthenium nanocatalysts supported on nitrogen-doped graphene aerogel and carbon nanotubes in Fischer-Tropsch synthesis, Arab. J. Chem. 16 (2023) 104914, https://doi.org/10.1016/j.arabjc.2023.104914.
[281] S. Taghavi, A. Asghari, A. Tavasoli, Chemical engineering research and design enhancement of performance and stability of graphene nano sheets supported cobalt catalyst in Fischer – Tropsch synthesis using graphene functionalization, Chem. Eng. Res. Des. 119 (2017) 198–208, https://doi.org/10.1016/j.cherd.2017.01.021.
[282] E.L. Wolf, Practical productions of graphene, supply and cost, Springe Mater. (2014) 19–38, https://doi.org/10.1007/978-3-319-03946-6_2.
[283] N. Asim, M. Badiei, N.A. Samsudin, M. Mohammad, H. Razali, S. Soltani, N. Amin, Application of graphene-based materials in developing sustainable infrastructure: an overview, Compos. Part B Eng. 245 (2022) 110188, https://doi.org/10.1016/j.compositesb.2022.110188.
[284] M.B. Burkholder, F.B.A. Rahman, E.H. Chandler, J.R. Regalbuto, B.F. Gupton, J. M.M. Tengco, Metal supported graphene catalysis: a review on the benefits of nanoparticular supported specialty sp2carbon catalysts on enhancing the activities of multiple chemical transformations, Carbon Trends 9 (2022), https://doi.org/10.1016/j.cartre.2022.100196.
[285] N.M. Julkapli, S. Bagheri, Graphene supported heterogeneous catalysts: an overview, Int. J. Hydrog. Energy 40 (2015) 948–979, https://doi.org/10.1016/j.ijhydene.2014.10.129.
[286] S.E. Lowe, Y.L. Zhong, Challenges of industrial-scale graphene oxide production, Graph. Oxide Fundam. Appl. (2016) 410–431, https://doi.org/10.1002/9781119069447.ch13.
[287] R.K. Singh, R. Kumar, D.P. Singh, Graphene oxide: strategies for synthesis, reduction and frontier applications, RSC Adv. 6 (2016) 64993–65011, https://doi.org/10.1039/c6ra07626b.
[288] A. Iqbal, S. Sajjad, S.A.K. Leghari, Low cost graphene oxide modified alumina nanocomposite as solar light induced photocatalyst, ACS Appl. Nano Mater. 1 (2018) 4612–4621, https://doi.org/10.1021/acsanm.8b00649.

[289] S.B. Singh, C.M. Hussain, Nano-graphene as groundbreaking miracle material: catalytic and commercial perspectives, ChemistrySelect 3 (2018) 9533–9544, https://doi.org/10.1002/slct.201802211.
[290] L. Serrano-Luján, S. Víctor-Román, C. Toledo, O. Sanahuja-Parejo, A.E. Mansour, J. Abad, A. Amassian, A.M. Benito, W.K. Maser, A. Urbina, Environmental impact of the production of graphene oxide and reduced graphene oxide, SN Appl. Sci. 1 (2019) 1–12, https://doi.org/10.1007/s42452-019-0193-1.
[291] X.J. Lee, B.Y.Z. Hiew, K.C. Lai, L.Y. Lee, S. Gan, S. Thangalazhy-Gopakumar, S. Rigby, Review on graphene and its derivatives: synthesis methods and potential industrial implementation, J. Taiwan Inst. Chem. Eng. 98 (2019) 163–180, https://doi.org/10.1016/j.jtice.2018.10.028.
[292] D.M. Chis, E.M. Crisan, A cost-benefit analysis of four graphene-based materials, Manag. Chall. Contemp. Soc. Proc. 14 (2021) 135–141.
[293] F. Mori, M. Kubouchi, Y. Arao, Effect of graphite structures on the productivity and quality of few-layer graphene in liquid-phase exfoliation, J. Mater. Sci. 53 (2018) 12807–12815, https://doi.org/10.1007/s10853-018-2538-3.